ACS Chemical Neuroscience

pubs.acs.org/chemneuro Research Article

Putative Synthetic Cannabinoids MEPIRAPIM, 5F-BEPIRAPIM (NNL-2), and Their Analogues Are T-Type Calcium Channel (Ca_V3) Inhibitors

Richard C. Kevin, Somayeh Mirlohi, Jamie J. Manning, Rochelle Boyd, Elizabeth A. Cairns, Adam Ametovski, Felcia Lai, Jia Lin Luo, William Jorgensen, Ross Ellison, Roy R. Gerona, David E. Hibbs, Iain S. McGregor, Michelle Glass, Mark Connor, Chris Bladen, Gerald W. Zamponi, and Samuel D. Banister*

Cite This: ACS Chem. Neurosci. 2022, 13, 1395−1409 Read Online

ACCESS | Metrics & More | Article Recommendations | Supporting Information

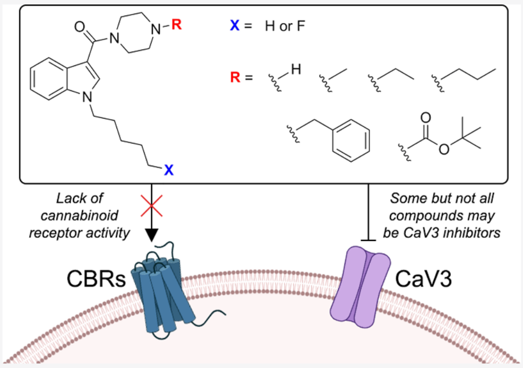

ABSTRACT: Synthetic cannabinoid receptor agonists (SCRAs) are a large and growing class of new psychoactive substances (NPSs). Two recently identified compounds, MEPIRAPIM and 5F-BEPIRAPIM (NNL-2), have not been confirmed as agonists of either cannabinoid receptor subtype but share structural similarities with both SCRAs and a class of T-type calcium channel (Ca_V3) inhibitors under development as new treatments for epilepsy and pain. In this study, MEPIRAPIM and 5F-BEPIRAPIM and 10 systematic analogues were synthesized, analytically characterized, and pharmacologically evaluated using *in vitro* cannabinoid receptor and Ca_V3 assays. Several compounds showed micromolar affinities for CB_1 and/or CB_2, with several functioning as low potency agonists of CB_1 and CB_2 in a membrane potential assay. 5F-BEPIRAPIM and four other derivatives were identified as potential Ca_V3 inhibitors through a functional calcium flux assay (>70% inhibition), which was further confirmed using whole-cell patch-clamp electrophysiology. Additionally, MEPIRAPIM and 5F-BEPIRAPIM were evaluated *in vivo* using a cannabimimetic mouse model. Despite detections of MEPIRAPIM and 5F-BEPIRAPIM in the NPS market, only the highest MEPIRAPIM dose (30 mg/kg) elicited a mild hypothermic response in mice, with no hypothermia observed for 5F-BEPIRAPIM, suggesting minimal central CB_1 receptor activity.

KEYWORDS: *cannabinoid, MEPIRAPIM, BEPIRAPIM, NNL, pharmacology, calcium channel*

■ INTRODUCTION

Synthetic cannabinoid receptor agonists (SCRAs) are a diverse class of new psychoactive substances (NPSs) that exert intoxication via activation of cannabinoid type 1 receptors (CB_1). Most SCRAs function as agonists of both cannabinoid receptor subtypes, CB_1 and CB_2, with some compounds exhibiting potencies and efficacies equal to or greater than conventional “full agonists” like CP 55,940.[1−3] The chemical evolution of SCRA NPS changes dynamically in response to local legislation,[4] requiring the ongoing development of reference standards and detection methods for emerging compounds.[5−11] Understanding structure−activity relationships for emergent SCRAs and their analogues facilitates more efficient allocation of resources to those SCRAs of greatest concern.

The earliest SCRAs were acylindoles such as JWH-018 (**1**; Figure 1) and XLR-11 (**2**), which possessed moderate potencies and efficacies at CB_1,[12] but as these compounds became prohibited in the United States and elsewhere, more potent and efficacious indole and indazole amides emerged in NPS markets to replace them.[13] More recent members of this class, such as amino acid-derived SCRAs AB-PINACA (**3**), ADB-CHMINACA (**4**), and AMB-FUBINACA (**5**), are frequently linked to mass intoxication events and serious adverse effects in the United States and other countries.[14−20] Owing to their rapid proliferation, many recent SCRAs are unknown in the scientific literature at the time of initial detection in NPS markets; cannabimimetic activity remains to be confirmed *in vitro* and *in vivo*.

The present study focuses on the synthesis and characterization of a series of compounds (**6**−**17**; Figure 2) including and closely related to MEPIRAPIM (**7**) and 5F-BEPIRAPIM (NNL-

Received: December 12, 2021
Accepted: March 22, 2022
Published: April 20, 2022

https://doi.org/10.1021/acschemneuro.1c00822
ACS Chem. Neurosci. 2022, 13, 1395−1409

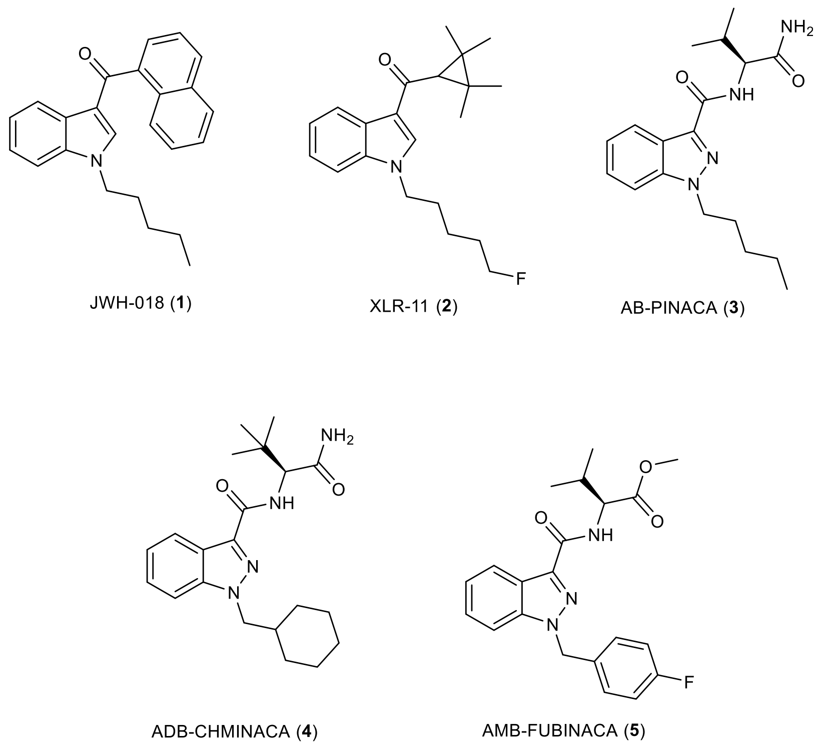

Figure 1. Synthetic cannabinoid receptor agonists (SCRAs) identified as new psychoactive substances.

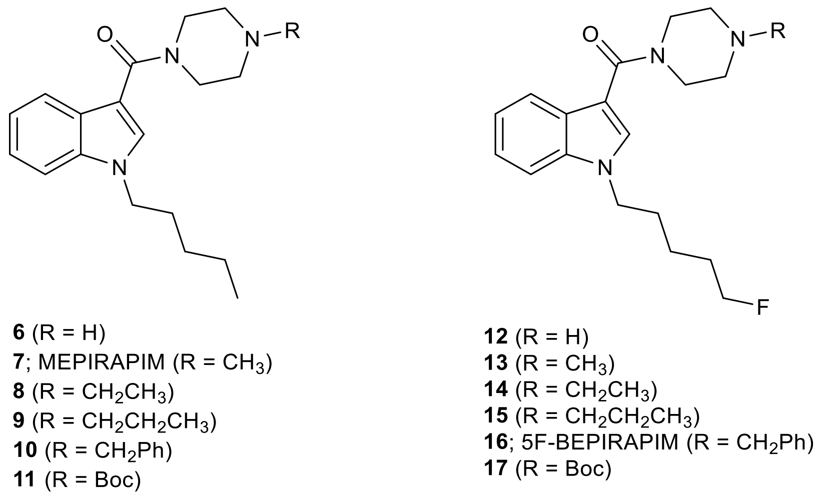

Figure 2. MEPIRAPIM, 5F-BEPIRAPIM (NNL-2), and their analogues.

2, **16**). MEPIRAPIM (**7**) was first reported as an NPS in Japan in 2013[21] and bears structural similarity to CB_1 and CB_2 agonists discovered by Organon International and later developed by Schering-Plough.[22,23] MEPIRAPIM has since been reported in other regions, and a fluorinated benzylic analogue, 5F-BEPIRAPIM (NNL-2, **16**), was recently identified in the seized material from a clandestine laboratory in China.[24−26] Very little is known about the pharmacology of this class of SCRAs, however, and MEPIRAPIM and acetylfentanyl were detected in two cases of fatal overdose.[27] In these cases, MEPIRAPIM was detected at much higher urine concentrations compared to typical levels for other SCRAs, which may suggest unusual pharmacokinetics or metabolism.[28]

MEPIRAPIM possesses low affinity for CB_1 (K_i = 2650 nM) and CB_2 (K_i = 1850 nM) receptors despite apparent design inspiration from optimized Organon International/Schering-Plough CB_1/CB_2 agonists such as Org 28611 (also known as SCH-900,111, **18**; Figure 3) and putative SCRA NPS like 5F-PY-PICA (**19**).[10,22,29] Org 28611 possesses high affinities for both CB_1 (K_i = 1.3 nM) and CB_2 receptors (K_i = 1.6 nM) and functions as a potent, high efficacy CB_1 receptor agonist (EC_{50} = 25 nM). Org 28611 demonstrated adequate drug metabolism and pharmacokinetic (DMPK) profiles *in vitro* and *in vivo*, good aqueous solubility (129 $mg \cdot L^{-1}$ at pH 6.9) and brain penetration, and was evaluated clinically as a potential intravenous analgesic agent.[22,30] By contrast, 5F-PY-PICA shows negligible affinity for CB_1 (K_i > 10,000 nM) and micromolar affinity for CB_2 receptors (K_i = 1737 nM) and functions as a selective CB_2 partial agonist (EC_{50} = 338 nM; E_{max} = 50%) with negligible effect on CB_1 (E_{max} = 12% at 10 μM).[29]

MEPIRAPIM also bears similarity to carbazoles designed to activate cannabinoid receptors and inhibit T-type calcium

https://doi.org/10.1021/acschemneuro.1c00822
ACS Chem. Neurosci. 2022, 13, 1395−1409

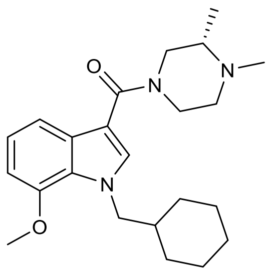

Org 28611 (**18**)

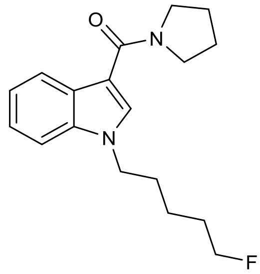

5F-PY-PICA (**19**)

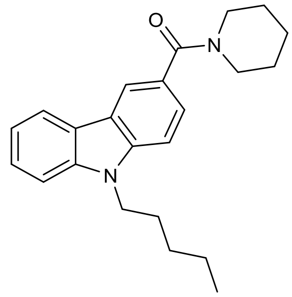

NMP-7 (**20**)

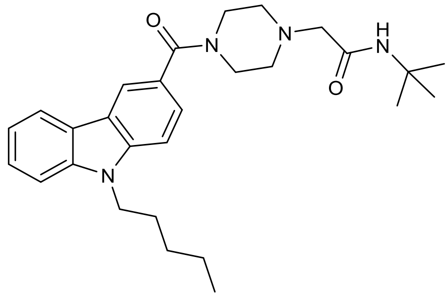

21

Figure 3. Analogues of MEPIRAPIM and 5F-BEPIRAPIM with diverse pharmacological profiles.

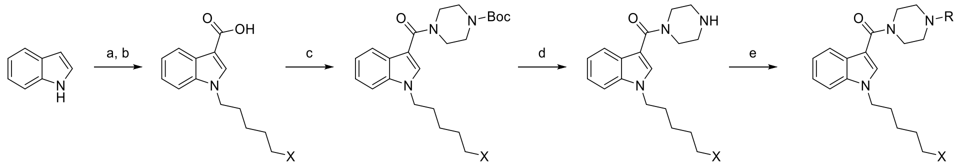

22

23 (X = H)
24 (X = F)

11 (X = H)
17 (X = F)

6 (X = H)
12 (X = F)

7 (X = H; R = CH_3)
8 (X = H; R = CH_2CH_3)
9 (X = H; R = $CH_2CH_2CH_3$)
10 (X = H; R = CH_2Ph)
13 (X = F; R = CH_3)
14 (X = F; R = CH_2CH_3)
15 (X = F; R = $CH_2CH_2CH_3$)
16 (X = F; R = CH_2Ph)

Figure 4. Reagents and conditions: (a) (i) NaH, $X(CH_2)_5Br$, *N*,*N*-dimethylformamide (DMF), 0 °C, rt, 1 h; (ii) $(CF_3CO)_2O$, 0 °C, rt, 1 h; (b) KOH, MeOH, PhMe, reflux, 2 h (**23**: 55%; **24**: 67%, over three steps); (c) Boc-piperazine, EDC·HCl, HOBt·H_2O, Et_3N, DMF, rt, 14 h (**11**: 92%; **17**: 89%); (d) 4 M HCl in dioxane, 0 °C, rt, 16 h (**6**·HCl: 91%; **12**·HCl: 84%); and (e) RCHO, $NaBH(OAc)_3$, $ClCH_2CH_2Cl$, rt, 2 h, 85–95%.

channels as dual mechanism analgesics, such as NMP-7 (**20**) and **21**.[31,32] T-type calcium channels (Ca_V3) are a subfamily of low-voltage-gated Ca^{2+} channels, with three subtypes defined by their α1 subunit, namely, $Ca_V3.1$ (α1G), $Ca_V3.2$ (α1H), and $Ca_V3.3$ (α1I).[33−36]

T-type calcium channels possess a number of unique biophysical properties, including small unitary conductance and rapid inactivation kinetics.[37] They also exhibit a hyperpolarized voltage dependence of activation and inactivation that give rise to a significant window current near typical neuronal resting membrane potentials.[38] These latter features allow T-type channels to efficiently regulate neuronal excitability by supporting both action potential initiation and rebound burst activity.[39] They also allow T-type channels to partake in the low threshold release of hormones and neurotransmitters.[40] Aberrant activation of T-type calcium channels has been linked to the development of conditions such as epilepsy and chronic pain, and genetic mutations in the three genes encoding the T-type channel family are associated with conditions such as epilepsy, neuromuscular diseases, primary aldosteronism, and autism.[41] It is thus not surprising that T-type calcium channels have emerged as pharmacological targets in the treatment of seizure disorders and are being explored as potential targets in the treatment of tremors (for review, see ref 42). Indeed, Ca_V3 inhibition is thought to be the key mechanism of action for the approved antiepileptic drugs zonisamide and ethosuximide, and Ca_V3 inhibitors Z944 and ACT-709,478 are currently in phase II clinical trials.[43,44] $Ca_V3.2$ T-type calcium channels are also considered as potential targets for chronic pain,[45] although the inhibitor ABT-639 has failed in a phase II trial.[46] Finally, there is emerging evidence that $Ca_V3.2$ channels may be a potential target for treating pruritus.[47,48] Hence, T-type channel inhibitors have considerable therapeutic potential, and it is important to identify novel pharmacophores that act on these channels for further optimization and development.[43]

Activation of CB_1 and CB_2 receptors produces analgesia in many animal models of nociception, through actions at sites in the central and peripheral nervous systems, as well as the immune system.[49] It has also been reported that modest CB_1 agonism can contribute to the analgesic effects of moderately selective CB_2 agonists in the complete Freund's adjuvant (CFA) model of inflammatory nociception[50] and that low occupancy of

https://doi.org/10.1021/acschemneuro.1c00822
ACS Chem. Neurosci. 2022, 13, 1395−1409

Table 1. Binding Affinities and Functional Activities of SCRAs 6−17 at hCB_1 and hCB_2 Receptors[a,b]

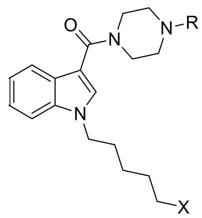

				hCB_1		hCB_2	
compound	X	R	calc cLogP	pK_i [M] ± SEM (K_i, μM)[a]	max ± SEM (% CP 55 940)[b]	pK_i [M] ± SEM (K_i, μM)[a]	max ± SEM (% CP 55 940)[b]
6	H	H	2.23	<5 (>10)	17.2 ± 13.7	<5 (>10)	9.8 ± 5.2
7	H	Me	2.60	<5 (>10)	40.0 ± 5.9	5.93 ± 0.02 (1.18)	16.9 ± 6.3
8	H	Et	2.94	<5 (>10)	37.0 ± 9.0	5.98 ± 0.03 (1.05)	13.1 ± 5.3
9	H	Pr	3.43	5.27 ± 0.08 (5.37)	9.8 ± 8.5	5.68 ± 0.08 (2.09)	15.9 ± 6.7
10	H	Bn	4.34	5.47 ± 0.07 (3.39)	17.7 ± 14.4	5.20 ± 0.13 (6.31)	15.5 ± 8.7
11	H	Boc	3.33	<5 (>10)	2.9 ± 1.0	<5 (>10)	3.8 ± 3.9
12	F	H	1.73	<5 (>10)	5.0 ± 8.2	<5 (>10)	16.7 ±11.1
13	F	Me	2.11	<5 (>10)	44.3 ± 5.9	<5 (>10)	16.4 ± 4.6
14	F	Et	2.45	<5 (>10)	35.1 ± 7.6	5.53 ± 0.08 (2.95)	15.7 ± 3.8
15	F	Pr	2.94	<5 (>10)	12.3 ± 12.1	<5 (>10)	23.8 ± 6.6
16	F	Bn	3.84	5.65 ± 0.07 (2.24)	0.5 ± 2.6	5.34 ± 0.13 (4.57)	8.2 ± 2.7
17	F	Boc	2.84	<5 (>10)	0.2 ± 0.5	<5 (>10)	5.4 ± 4.3

[a] pK_i < 5 indicates less than 60% displacement of [^{3}H]ligand at 10 μM in a binding assay. [b] Maximum response in the functional membrane potential assay at 10 μM compared to that at 1 μM CP 55,940 (100%). cLog *P* computed using ChemDraw (version 20).

CB_1 by an agonist with low intrinsic efficacy results in antinociception.[51] Combined, these data suggest that compounds with low efficacy CB receptor agonism and potent T-type channel inhibition could be effective analgesics.

The activities of MEPIRAPIM, 5F-BEPIRAPIM, and related compounds at CB receptors have not yet been defined *in vitro* or *in vivo* and, as indicated above, there seemed to be a possibility that they could also have activity at Ca_V3 channels. To address whether MEPIRAPIM, 5F-BEPIRAPIM, and related compounds are SCRAs and/or T-type calcium channel modulators, we devised a library of analogues based on the systematic modification of the pendant alkyl group to incorporate a homologous series from methyl to propyl substituents, as well as unsubstituted, *tert*-butyl carbamate-protected, and benzyl-substituted examples (see **6**−**17**; Figure 2). Here, we report the synthesis, analytical chemistry, and *in vitro* cannabinoid and T-type calcium channel pharmacology of **6**−**17** and identify important structure−activity relationships (SARs) that could be used for further development and optimization of these pharmacophores. Additionally, MEPIRAPIM and 5F-BEPIRAPIM, which have been detected in NPS products, were assessed for *in vivo* cannabinoid activity using radiobiotelemetry in mice.

■ RESULTS AND DISCUSSION

The synthesis of compounds **6**−**17** is shown in Figure 4. Indole (**22**) was alkylated with either bromopentane or 5-fluorobromopentane and treated with trifluoroacetic anhydride to give the corresponding trifluoroacetyl indoles, hydrolysis of which afforded carboxylic acids **23** or **24**, respectively. Coupling of **23** or **24** with Boc-piperazine using 1-ethyl-3-(3′-dimethylaminopropyl)carbodiimide (EDC) gave **11** and **17**, which were deprotected using hydrogen chloride in dioxane to give piperazines **6** and **12** as their hydrochloride salts. Reductive alkylation of **6** or **12** with either formaldehyde, acetaldehyde, propanal, or benzaldehyde in the presence of sodium triacetoxyborohydride afforded **7**−**10** and **13**−**16** in excellent yield. The free base amines were purified by flash chromatography and characterized by NMR spectroscopy. The free base amines were then converted to their hydrochloride salts and purified by recrystallization and subjected to *in vitro* binding and functional activity assays at CB_1 and CB_2 receptors and *in vitro* functional activity assays at $Ca_V3.1$, $Ca_V3.2$, and $Ca_V3.3$ channels.

Ligands **6**−**17** were subjected to competition radioligand binding assays and fluorescence-based membrane potential assays at human CB_1 and CB_2 receptors (Table 1). Most compounds showed low or negligible affinities for CB_1 and CB_2 receptors, with K_i values generally not determined (i.e., pK_i < 5, <60% displacement of radioligand at 10 μM). CB_1 binding was greatest for derivatives featuring a pendant propyl (**9**: K_i = 5.37 μM) or benzyl group (**10**: K_i = 3.39 μM; **16**: K_i = 2.24 μM) on the terminal piperazine nitrogen, suggesting a minimum steric requirement in this region for CB_1 binding. Fluorination had no major influence on CB_1 binding, with **10** showing a similar K_i value to the corresponding fluorinated compound, **16**. CB_2 binding favored smaller piperazine substituents, with the highest affinities observed for the *N*-methyl (**7**: K_i = 1.18 μM) and *N*-ethyl analogues (**8**: K_i = 1.05 μM) in the desfluoro series and decreasing for the *N*-propyl (**9**: K_i = 2.09 μM) and *N*-benzyl (**10**: K_i = 6.31 μM) cases. In the corresponding fluorinated congeners, K_i values were only determinable for the ethyl (**14**) and benzyl cases (**16**) and not for the methyl (**13**) or propyl (**15**) derivatives. In both fluorinated and nonfluorinated series, neither an unsubstituted (**6** and **12**) nor a *tert*-butyl carbamate-protected (**11** and **17**) piperazine was tolerated for CB_1 or CB_2 binding.

In terms of functional activity at CB_1 and CB_2, all compounds demonstrated negligible or low potency agonist activity, which was not surprising given the low affinity for these receptors. It was not possible to determine EC_{50} values; at 10 μM, all compounds produced only limited CB_1 or CB_2 receptor

https://doi.org/10.1021/acschemneuro.1c00822
ACS Chem. Neurosci. 2022, 13, 1395−1409

activation compared to a maximally efficacious concentration of CP 55,940 (1 μM; 100%). For CB_1, receptor activation ranged from approximately 0 to 44% of maximum response after normalization and approximately 4−49% of maximum for CB_2. Overall, several compounds appear to have some CB_1 and/or CB_2 agonist activity, albeit with apparent low potency compared to other recent generation SCRAs.[52] It was not possible to infer meaningful SARs for **6−17** given broadly similar low potency across all compounds.

The calcium channel activity of **6−17** was investigated using a fluorometric imaging plate-reader (FLIPR) calcium flux assay in $Ca_V3.1$-, $Ca_V3.2$-, and $Ca_V3.3$-transfected cells, and the data are shown in Table 2 and plotted in Figure 5, with representative traces included in Supporting Figure S20. Figure 5 shows results of SCRAs screened at 10 μM in the calcium flux assay on stably expressed human T-type calcium channels in HEK293T cells ($Ca_V3.1$, $Ca_V3.2$, and $Ca_V3.3$). Inhibition induced by the nonselective Ca_V3 inhibitor NNC 55-0396 (NNC; 10 μM) was included as a positive control. The functional calcium flux assay identified five compounds that potently inhibited (>70%, italic values in Table 2) the calcium response for one or more Ca_V3 subtype: **9**, **10**, **11**, **16**, and **17**. Appreciable $Ca_V3.1/3.2$ inhibition was achieved for compounds with R = Bn (i.e., **10** and **16**) or R = Boc (i.e., **11** and **17**), regardless of compounds possessing a pentyl chain (X = H) or a 5-fluoropentyl group (X = F), suggesting that terminal fluorination does not influence $Ca_V3.1/3.2$ inhibition with these pendant R-groups. Conversely, comparing **8** and **14** (R = Et) or **9** and **15** (R = Pr), terminal fluorination substantially reduces activity across all Ca_V subtypes.

Table 2. Mean Calcium Fluorescence Inhibition at $Ca_V3.1$, $Ca_V3.2$, and $Ca_V3.3$ by Compounds 6−17 and NNC Using a Functional Calcium Flux Assay

			% fluorescence inhibition ± SEM		
compound	X	R	$Ca_V3.1$	$Ca_V3.2$	$Ca_V3.3$
NNC 55- 0396			78.5 ± 5.1	85.2 ± 3.1	94.2 ± 1.9
6	H	H	28.3 ± 12.3	38.7 ± 11.8	28.4 ± 6.6
7	H	Me	40.9 ± 8.1	42.6 ± 9.9	29.1 ± 5.8
8	H	Et	48.0 ± 7.1	45.7 ± 4.6	66.9 ± 8.3
9	H	Pr	*78.9 ± 5.9*	67.6 ± 5.2	*76.0 ± 7.4*
10	H	Bn	*79.5 ± 7.6*	*74.0 ± 8.2*	55.6 ± 7.4
11	H	Boc	*92.7 ± 2.3*	*88.2 ± 4.7*	5.1 ± 0.8
12	F	H	31.2 ± 6.5	21.4 ± 7.1	2.3 ± 4.2
13	F	Me	36.1 ± 7.7	29.6 ± 11.5	14.2 ± 5.8
14	F	Et	1.8 ± 3.9	4.5 ± 5.5	14.1 ± 6.9
15	F	Pr	43.7 ± 8.4	21.4 ± 7.1	6.6 ± 4.5
16	F	Bn	*92.2 ± 2.5*	*74.5 ± 6.6*	*87.5 ± 6.6*
17	F	Boc	*96.0 ± 1.3*	*95.5 ± 1.1*	26.8 ± 10.6

Notably, both **11** and its corresponding fluorinated derivative **17** feature the *tert*-butyl carbamate moiety on the piperazine ring and showed a similar profile, with selective inhibition of $Ca_V3.1$ (93% and 96%, respectively) and $Ca_V3.2$ (88% and 96%, respectively) but not $Ca_V3.3$. Strong $Ca_V3.2$ inhibition was also achieved by carbazole analogues,[32] indicating that the choice of carbazole or indole core is not a critical determinant of the $Ca_V3.2$ channel blockade. Only two compounds, **9** (X = H, R = Pr) and **16** (X = F, R = Bn), produced strong (>70%) inhibition of $Ca_V3.3$, suggesting that a more complex interaction between terminal fluorination and R-group is necessary for strong inhibition of this channel subtype in the calcium flux assay.

To confirm Ca_V3 inhibition by the more active compounds (**9**, **10**, **11**, **16**, and **17**), follow-up electrophysiology experiments were carried out (Figure 6; Supporting Figure S21). As compounds with little inhibitory activity display similarly low activity in electrophysiology experiments,[53] compounds **6**, **7**, **8**, **12**, **13**, **14**, and **15** were not tested in this platform. Compounds **9**, **10**, **11**, **16**, and **17** showed the inhibition of current for each of $Ca_V3.1$, $Ca_V3.2$, and $Ca_V3.3$, with, generally, slightly reduced inhibitory values compared to the calcium assay data. The greatest inhibition differences between the two assays were observed for $Ca_V3.3$, suggesting that the predictive utility of the calcium assay system is less robust for this subtype. For example, compared to the fluorescence inhibition in the calcium flux assay experiments, current inhibition at $Ca_V3.3$ decreased slightly for **9**

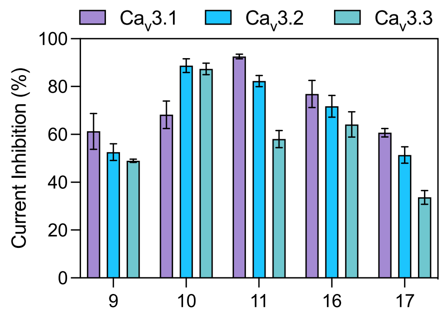

Figure 6. Mean current inhibition at $Ca_V3.1$, $Ca_V3.2$, and $Ca_V3.3$ by compounds **9−11**, **16**, and **17** using patch-clamp electrophysiology. Data are % current inhibition at 10 μM and represent the mean ± SEM of six independent whole-cell patch-clamp recordings per compound on each stably expressed ion channel.

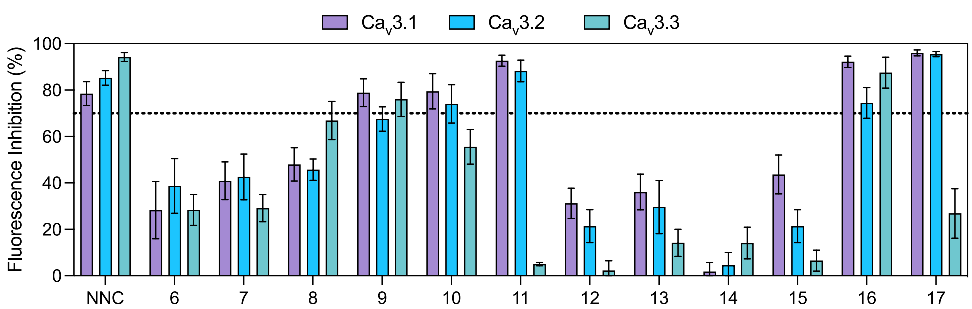

Figure 5. Mean fluorescence inhibition at $Ca_V3.1$, $Ca_V3.2$, and $Ca_V3.3$ by compounds **6−17** and positive control NNC 55-0396 (NNC; Supporting Figure S22) using a functional calcium flux assay. Data are % fluorescence inhibition at 10 μM and represent the mean ± standard error of the mean (SEM) of six independent experiments per compound.

https://doi.org/10.1021/acschemneuro.1c00822
ACS Chem. Neurosci. 2022, 13, 1395−1409

and **16**, increased for **10** and **11**, and was consistent/unchanged for **17**. This had the effect of abolishing any observed Ca_V3 subtype selectivity suggested by the calcium flux assay data.

Overall, **9**, **10**, **11**, **16**, and **17** are efficacious inhibitors of $Ca_V3.1$, $Ca_V3.2$, and $Ca_V3.3$, with little selectivity between the subtypes. Several of these compounds, in particular, **11** and **17**, are structurally similar to cannabinoids shown to mediate potent analgesic responses *in vivo* via $Ca_V3.2$,[31,32] whereas **9**, **10**, and **16** have important steric and electronic differences.

The observed differences between the results of the electrophysiology and functional assays on $Ca_V3.3$ could be due to the much slower kinetics of this subtype versus $Ca_V3.1$ and $Ca_V3.2$. Given the depolarized resting membrane potential (Vm) of HEK cells (approximately −60 mV), the functional assay may detect more inactivated state inhibition compared to the electrophysiology assay that holds cells artificially at −100 mV. Therefore, any putative inactivated state blocking component could be diminished and lead to changes in both apparent affinity and subtype dependence. To help mitigate this, low potassium HBSS was used in the calcium flux assay to keep the Vm of the cells at more negative potentials. In addition, depolarization of the membrane in the calcium flux assay was created by the addition of 10 mM Ca^{2+}, versus a voltage step protocol to −30 mV, to open the expressed channel subtype. Determination of whether the addition of the relatively high concentration of Ca^{2+}, versus 5 mM Ba^{2+} in the electrophysiology assay, contributes to the observed differences in $Ca_V3.3$ inhibition in the two assays would require detailed kinetic experiments that are beyond the scope of the current study.

MEPIRAPIM (**7**) and 5F-BEPIRAPIM (**16**) have been detected in the NPS market as putative SCRAs based on structural motifs common in other SCRAs. It was therefore hypothesized that these two compounds might possess cannabimimetic activities *in vivo*. In rodents, centrally active CB_1 receptor agonists produce hypothermia, hypolocomotion, and bradycardia that are typically concordant with the central cannabinoid activity in humans,[11,54−57] and these effects may be used as a proxy for potential psychoactivity. To explore the potential cannabimimetic effects of these SCRAs *in vivo*, the effect of MEPIRAPIM and 5F-BEPIRAPIM on core body temperature was evaluated in mice using radiobiotelemetry (Figure 7). No hypothermic effects were observed except for a modest and brief effect after the administration of 30 mg/kg MEPIRAPIM (AUC: $t(3) = 3.82$, $p = .02$). Compared to other recent generation SCRAs tested using this model, which produce pronounced hypothermic effects (exceeding −5 °C from baseline) at doses as low as 0.3 mg/kg,[1,3,11,54] MEPIRAPIM and 5F-BEPIRAPIM appear to possess relatively poor cannabimimetic efficacy in mice. However, this is entirely consistent with their *in vitro* pharmacological profiles at CB_1 (and CB_2) and mirrors our observations for other putative SCRA NPSs that possess comparably poor binding/agonist efficacy at CB_1, e.g., 5F-PY-PICA or AB-001.[29,58]

To gain a better understanding of the SARs underlying cannabinoid receptor binding, compounds **7**, **9**, **10**, **14**, **16**, and Org 28611 were selected for induced fit docking in CB_1 (PDB: 6N4B) and CB_2 (PDB: 6PT0) receptors. The compounds share almost identical binding poses at both receptors, which is not surprising considering that the agonist-binding pockets of CB_1 and CB_2 receptors are very similar in nature.[59] In CB_1 receptors, the indole core makes π−π interactions with Phe268 and/or Phe200. The carbonyl group makes the H-bond interaction with Ser383, and the tail group sits in the side pocket formed by Leu193, Thr197, Thr275, Ile271, Trp276, and Met363. The alkyl substituent at the piperazine ring makes hydrophobic interactions with Lys192, Phe177, and Phe189, whereas compounds **10** and **16**, with a benzene substituent, also form π−π interaction with Phe177 and Phe189.

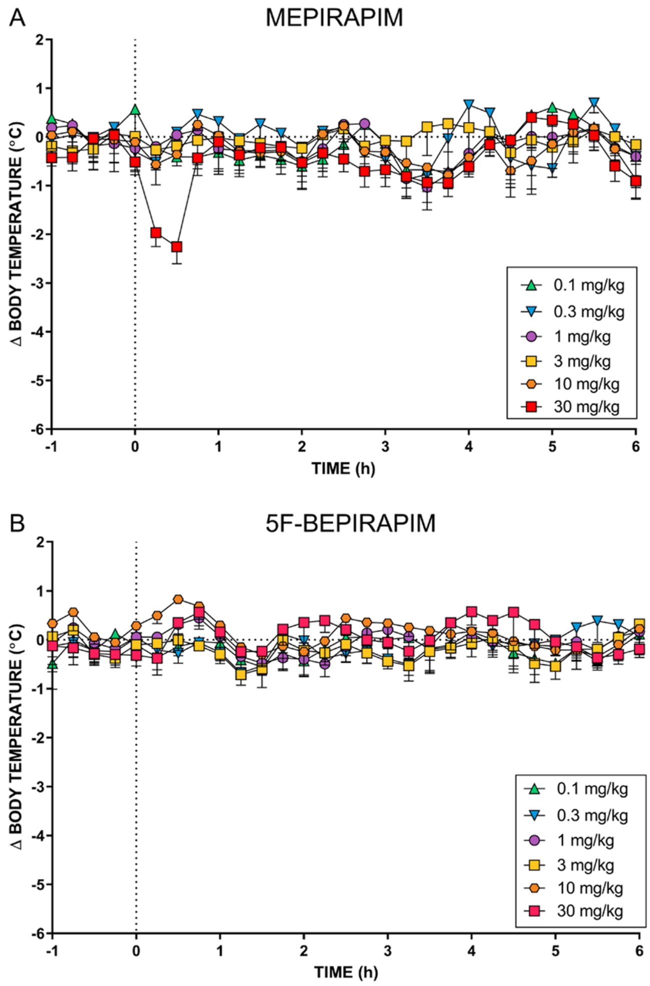

Figure 7. Change in body temperature following the intraperitoneal injection of (A) MEPIRAPIM and (B) 5F-BEPIRAPIM relative to a baseline vehicle injection. The vertical dashed line denotes the time of injection, and each data point represents the mean (±SEM) change in body temperature of four mice.

Similarly, in the CB_2 receptor, the indole ring makes π−π interactions with Phe117 and/or Phe183, and the carbonyl group makes H-bond interaction with Ser285. The tail group now sits in the hydrophobic pocket that is surrounded by Thr114, Phe183, Tyr190, Leu191, Leu193, Trp194, and Met265. The substituents at the piperazine ring interact with hydrophobic residues Phe94, Phe106, and Ile110, and the benzene ring of compounds **10** and **16** also makes π−π interactions with Phe94.

Sitemap[60,61] analysis of the CB_1 and CB_2 orthosteric binding sites shows that the CB_2 receptor has a much smaller binding site volume (284.69 Å^3) than the CB_1 receptor (502.50 Å^3).

Compound **7** (MEPIRAPIM) and Org 28611 were directly compared in the CB_1 receptor to identify why MEPIRAPIM is relatively inactive at CB_1 compared to Org 28611 (**18**) despite a number of structural similarities. Compared to **7**, Org 28611 has a methyl substitution at the 3-position of the piperazine ring and

https://doi.org/10.1021/acschemneuro.1c00822
ACS Chem. Neurosci. 2022, 13, 1395−1409

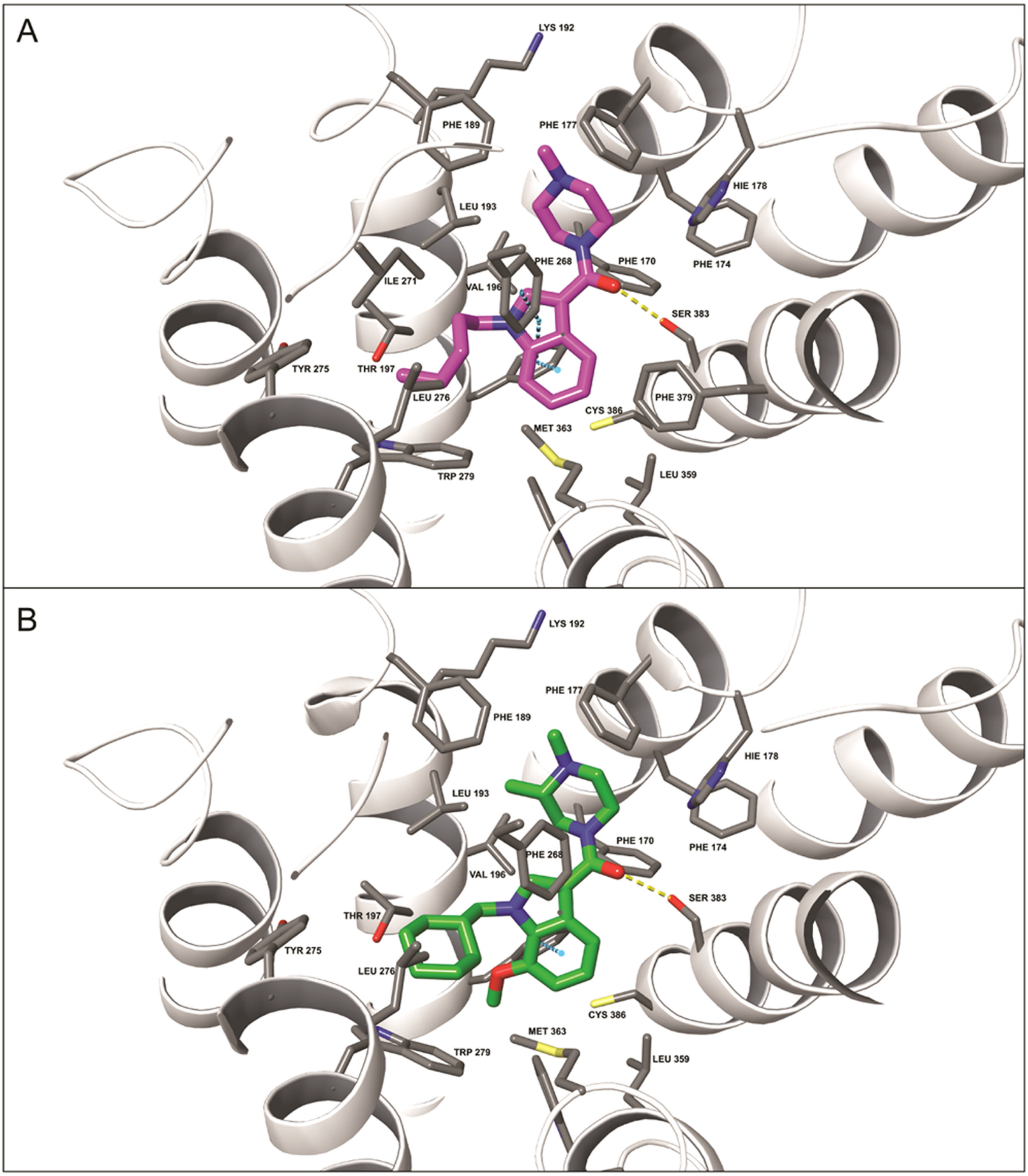

Figure 8. Docking simulation at CB_1 receptors for (A) MEPIRAPIM (7) and (B) Org 28611. Hydrophobic contacts between Leu193/Val196 and the methyl substituent of Org 28611 (**18**) appear to be a key determinant of the CB_1 receptor binding strength.

a methoxy substituent at the 6-position of the indole ring. No interactions between the methoxy group and the binding site were observed in the docking analysis. The methyl substituent of the piperazine ring of Org 28611 made hydrophobic contacts with Leu193 and Val196 and appeared to be responsible for the difference in potency between the two compounds (Figure 8). A methyl group at the 3- or 5-position of the piperazine ring is reported to improve potency,[62] and our previous work has also shown that SCRAs that interact with these two residues may give rise to stronger binding affinity to the receptor.[63] The IFD score, which indicates binding affinity, shows that Org 28611 has a stronger binding affinity to both the CB_1 receptors compared to compound 7 (−9744.10 and −9726.62 kcal/mol, respectively).

https://doi.org/10.1021/acschemneuro.1c00822
ACS Chem. Neurosci. 2022, 13, 1395−1409

■ CONCLUSIONS

Based on recent detections of MEPIRAPIM and 5F-BEPIRAPIM in drug markets and due to their structural similarities to known Ca_V3 inhibitors, we tested a library of MEPIRAPIM and 5F-BEPIRAPIM analogues for cannabinoid receptor and Ca_V3 activity. All tested compounds possessed low or negligible potency and efficacy at CB_1 and CB_2 receptors in vitro. A subset of compounds (**9**, **10**, **11**, **16**, and **17**) showed broad inhibition of Ca_V3 channels, with terminal fluorination having minimal impact on Ca_V3 activity or subtype selectivity, as measured by patch-clamp electrophysiology. Interestingly, Bladen et al. (2015) demonstrated that the related carbazole compound DX332 (Supporting Figure S23) had no activity on CB_1 and CB_2 and other carbazole derivatives in this series also did not interact strongly with CB_1 and CB_2. However, in the series of carbazole derivatives described by You et al. (2011), CB receptor interactions were observed. Together with the present study, these reports indicate that both indole and carbazole derivatives can have mixed Cav3/CB receptor activity and that the substituents in the R position (Figure 2) are more critical for determining whether a compound acts on Ca_V3, CBRs, or both. Further exploration and optimization of these compound classes may be warranted to develop an effective combined CBR agonist and Ca_V3 inhibitor.

The poor *in vivo* potency and efficacy of MEPIRAPIM and 5F-BEPIRAPIM, as compared to recent generation carboxamide-type SCRAs, suggest limited psychoactivity in humans, which appears to be at odds with the detection of these compounds in the NPS market. However, this is not the first time that apparently nonpsychoactive SCRAs have been detected. We previously reported that 5F-PY-PICA and 5F-PY-PINACA, detected in drug markets in 2015, possessed low binding affinity and efficacy at CB_1 receptors and that they failed to produce hypothermic effects in mice.[29] A potential explanation for this phenomenon is poor or absent pharmacological assessment in illicit/clandestine SCRA development production. Since clandestine NPS producers are unlikely to be systematically testing new scaffold-hopping compounds for CB_1 activity *in vitro* or *in vivo*, from time to time, unexpectedly low efficacy compounds may be introduced into the NPS market. However, we cannot exclude the possibility that these compounds could exert psychoactive effects by noncannabinoid-mediated mechanisms.

■ METHODS

General Chemical Synthesis Details. All reactions were performed under an atmosphere of nitrogen unless otherwise specified. All reagents, reactants, and solvents were obtained from Sigma-Aldrich (St. Louis, MO) and used as purchased. Analytical thin-layer chromatography was performed using Merck aluminum-backed silica gel 60 F254 (0.2 mm) plates (Merck, Darmstadt, Germany), which were visualized using shortwave (254 nm) UV fluorescence. Flash chromatography was performed using a Biotage Isolera Spektra One and Biotage SNAP KP-Sil silica cartridges (Uppsala, Sweden), with gradient elution terminating at the solvent combination indicated for each compound (*vide infra*). Melting point ranges (m.p.) were measured in open capillaries using a Stuart SMP50 Automated melting point apparatus (Cole-Palmer, Staffordshire, U.K.) and are uncorrected. Nuclear magnetic resonance spectra were recorded at 298 K using an Agilent 400 MHz spectrometer (Santa Clara, CA). The data are reported as chemical shift (δ ppm) relative to the residual protonated solvent resonance, multiplicity (s = singlet, br s = broad singlet, d = doublet, br d = broad doublet, t = triplet, q = quartet, quin. = quintet, m = multiplet), coupling constants (J Hz), relative integral, and assignment. High-resolution mass spectrometry (HRMS) data were collected using an Agilent LC 1260-QTOF-MS 6550 (Santa Clara, CA) or a Thermo Scientific Q Exactive HF-X hybrid quadrupole-orbitrap mass spectrometer (Waltham, MA). A methanolic extract of each pure standard was run using an electrospray ionization source in an automated MS/MS (information-dependent acquisition) mode. Accurate mass for the parent ion and its corresponding mass error expressed in parts per million (ppm) is reported.

*General Procedure for the Synthesis of (4-Alkylpiperazin-1-yl)(1-alkyl-1H-indol-3-yl)methanones (**7**−**10** and **13**−**16**).* To a solution of the free base of the appropriate (piperazin-1-yl)(1-alkyl-1*H*-indol-3-yl)methanone (**6** or **12**, 1 mmol) in 1,2-dichloroethane (3.5 mL) was added the appropriate aldehyde (1 mmol, 1.0 equiv), followed by sodium triacetoxyborohydride (297 mg, 1.4 mmol mmol, 1.4 equiv) in a single portion and the mixture was stirred at ambient temperature for 2 h. The reaction was quenched by the addition of 1 M aq. NaOH (3.5 mL), and the layers were separated. The aqueous phase was extracted with CH_2Cl_2 (3 × 3.5 mL), and the combined organic layers were washed with brine (10 mL), dried (Na_2SO_4), and the solvent was evaporated under reduced pressure. The crude products were purified by flash chromatography, converted to their hydrochloride salts, and recrystallized for pharmacological evaluation. Analytical data were obtained for each compound as the hydrochloride salt (M.p., HRMS) or as the free base liberated from the corresponding salt by dissolution in H_2O, adjusting the pH to 14 (1 M aq. NaOH), extracting with CH_2Cl_2 (and drying the extracts over Na_2SO_4), evaporating the solvent under reduced pressure, and drying the resultant oil under high vacuum (R_f, ^{1}H, and ^{13}C NMR).

*(4-Methylpiperazin-1-yl)(1-pentyl-1H-indol-3-yl)methanone Hydrochloride (**7**·HCl, MEPIRAPIM·HCl).* Subjecting **6** (300 mg, 1.00 mmol) and 37% aqueous formaldehyde (80 μL, 1.00 mmol, 1.0 equiv) to the procedure described above with additional sodium triacetoxyborohydride (848 mg, 4.00 mmol, 4.0 equiv)[64] gave, following purification by flash chromatography (CH_2Cl_2-MeOH, 90:10), **7** as a colorless oil (278 mg, 89%). The free base was converted to the hydrochloride and recrystallized from EtOAc to give a white solid. M.p. (HCl) 184−186 °C; R_f (free base) 0.14 (CH_2Cl_2-MeOH, 95:5); ^{1}H NMR (400 MHz, $CDCl_3$, free base): δ 7.71−7.68 (m, 1H), 7.46 (s, 1H), 7.35−7.70 (m, 1H), 7.18−7.27 (m, 2H), 4.12 (t, J = 7.2 Hz, 2H, NCH_2), 3.75 (t, J = 4.8 Hz, 4H, 2 × NCH_2), 2.45 (t, J = 4.8 Hz, 4H, 2 × NCH_2), 2.33 (s, 3H, NCH_3), 1.86 (quin., J = 7.2 Hz, 2H, CH_2), 1.30−1.38 (m, 4H, 2 × CH_2), 0.89 (t, J = 7.2 Hz, 3H, CH_3); ^{13}C NMR (100 MHz, $CDCl_3$, free base): δ 166.9 (CO), 135.9 (quat.), 130.8 (CH), 126.3 (quat.), 122.4 (CH), 120.9 (CH), 120.8 (CH), 110.5 (quat.), 110.1 (CH), 55.4 (2 × NCH_2), 46.9 (NCH_2), 46.3 (NCH_3), 45.4 (br, 2 × NCH_2), 30.0 (CH_2), 29.2 (CH_2), 22.4 (CH_2), 14.1 (CH_3); HRMS (ESI) $C_{19}H_{27}N_3O$ exact mass 313.2154, accurate mass 313.2158 (mass error 1.09 ppm).

*(4-Ethylpiperazin-1-yl)(1-pentyl-1H-indol-3-yl)methanone Hydrochloride (**8**·HCl).* Subjecting **6** (300 mg, 1.00 mmol) and acetaldehyde (56 μL, 1.00 mmol, 1.0 equiv) to the general procedure gave, following purification by flash chromatography (CH_2Cl_2-MeOH, 90:10), **8** as a colorless oil (304 mg, 93%). The free base was converted to the hydrochloride and recrystallized from EtOAc to give a white solid. M.p. (HCl) 165−167 °C; R_f (free base) 0.15 (CH_2Cl_2-MeOH, 95:5); ^{1}H NMR (400 MHz, $CDCl_3$, free base): δ 7.46 (s, 1H), 7.34−7.37 (m, 1H), 7.23−7.27 (m, 1H), 7.20 (m, 1H), 4.12 (t, J = 7.2 Hz, 2H, NCH_2), 3.76 (t, J = 4.8 Hz, 4H, 2 × CH_2), 2.44−2.51 (m, 6H, 3 × CH_3), 1.87 (quin., J = 7.2 Hz, 2H, CH_2), 1.03−1.38 (m, 4H, 2 × CH_2), 1.11 (t, J = 7.2 Hz, 3H, CH_2), 0.89 (t, J = 7.2 Hz, 3H, CH_3); ^{13}C NMR (100 MHz, $CDCl_3$, free base): δ 166.8 (CO), 136.0 (quat.), 130.8 (CH), 126.3 (quat.), 122.3 (CH), 120.8(8) (CH), 120.8(6) (CH), 110.6 (quat.), 110.1 (CH), 53.3 (2 × NCH_2), 52.5 (NCH_2), 46.9 (NCH_2), 29.9 (CH_2), 29.2 (CH_2), 22.4 (CH_2), 14.1 (CH_3), 12.1 (CH_3) (one missing or overlapping); HRMS (ESI) $C_{20}H_{29}N_3O$ exact mass 327.2311, accurate mass 327.2309 (mass error −0.40 ppm).

*(4-Propylpiperazin-1-yl)(1-pentyl-1H-indol-3-yl)methanone Hydrochloride (**9**·HCl).* Subjecting **6** (300 mg, 1.00 mmol) and propanal (72 μL, 1.00 mmol, 1.0 equiv) to the general procedure gave, following purification by flash chromatography (CH_2Cl_2-MeOH, 95:5), **9** as a

https://doi.org/10.1021/acschemneuro.1c00822
ACS Chem. Neurosci. 2022, 13, 1395−1409

colorless oil (290 mg, 85%). The free base was converted to the hydrochloride and recrystallized from EtOAc to give a white solid. M.p. (HCl) 102−105 °C; R_f (free base) 0.20 (CH_2Cl_2-MeOH, 95:5); ^{1}H NMR (400 MHz, DMSO-d_6, free base): δ 7.79 (s, 1H), 7.73−7.75 (m, 1H), 7.55−7.57 (m, 1H), 7.23 (ddd, J = 8.3, 7.0, 1.2 Hz, 1H), 7.15 (ddd, J = 8.0, 7.0, 1.0 Hz, 1H), 4.37 (br d, J = 14.0 Hz, 2H, CH_2), 4.22 (t, J = 7.2 Hz, 2H, NCH_2), 3.46−3.51 (m, 4H, 2 × CH_2), 3.02−3.09 (m, 4H, 2 × CH_2), 1.67−1.82 (m, 4H, 2 × CH_2), 1.18−1.35 (m, 4H, 2 × CH_2), 0.91 (t, J = 7.2 Hz, 3H, CH_3), 0.84 (t, J = 7.2 Hz, 3H, CH_3); ^{13}C NMR (100 MHz, DMSO-d_6, free base): δ 165.8 (CO), 136.1 (quat.), 132.3 (CH), 126.9 (quat.), 122.6 (CH), 121.1 (CH), 120.9 (CH), 111.0 (CH), 108.0 (quat.), 57.5 (NCH_2), 51.2 (2 × NCH_2), 46.3 (NCH_2), 41.6 (2 × NCH_2), 29.8 (CH_2), 28.8 (CH_2), 22.2 (CH_2), 17.1 (CH_2), 14.3 (CH_3), 11.4 (CH_3); HRMS (ESI) $C_{21}H_{31}N_3O$ exact mass 341.2467, accurate mass 341.2467 (mass error −0.14 ppm).

*(4-Benzylpiperazin-1-yl)(1-pentyl-1H-indol-3-yl)methanone Hydrochloride (**10**·HCl).* Subjecting **6** (300 mg, 1.00 mmol) and benzaldehyde (102 μL, 1.00 mmol, 1.0 equiv) to the general procedure gave, following purification by flash chromatography (CH_2Cl_2-MeOH, 95:5), **10** as a colorless oil (370 mg, 95%). The free base was converted to the hydrochloride and recrystallized from MeOH-Et_2O to give a white solid. M.p. (HCl) 219−221 °C; R_f (free base) 0.38 (CH_2Cl_2-MeOH, 95:5); ^{1}H NMR (400 MHz, $CDCl_3$, free base): δ 7.69−7.72 (m, 1H), 7.44 (s, 1H), 7.30−7.36 (m, 5H), 7.17−7.28 (m, 3H), 4.11 (t, J = 7.2 Hz, 2H, NCH_2), 3.74 (t, J = 4.8 Hz, 4H, 2 × CH_2), 3.55 (s, 2H, C$\underline{H}_2$Ph), 2.50 (t, J = 4.8 Hz, 4H, 2 × CH_2), 1.86 (quin., J = 7.2 Hz, 2H, CH_2), 1.26−1.41 (m, 4H, 2 × CH_2), 0.89 (t, J = 6.8 Hz, 3H, CH_3); ^{13}C NMR (100 MHz, $CDCl_3$, free base): δ 166.8 (CO), 137.9 (quat.), 135.9 (quat.), 130.7 (CH), 129.3 (2 × CH), 128.4 (2 × CH), 127.3 (CH), 126.3 (quat.), 122.3 (CH), 120.9 (CH), 120.8 (CH), 110.6 (quat.), 110.0 (CH), 63.1 ($\underline{C}H_2$Ph), 53.5 (2 × NCH_2), 46.8 (NCH_2), 45.5 (2 × NCH_2), 29.9 (CH_2), 29.2 (CH_2), 22.4 (CH_2), 14.1 (CH_3); HRMS (ESI) $C_{25}H_{31}N_3O$ exact mass 389.2467, accurate mass 389.2469 (mass error 0.40 ppm).

*(4-Methylpiperazin-1-yl)(1-(5-fluoropentyl)-1H-indol-3-yl)-methanone Hydrochloride (**13**·HCl).* Subjecting **12** (317 mg, 1.00 mmol) and 37% aqueous formaldehyde (80 μL, 1.00 mmol, 1.0 equiv) to the procedure described above with additional sodium triacetoxyborohydride (848 mg, 4.00 mmol, 4.0 equiv)[64] gave, following purification by flash chromatography (CH_2Cl_2-MeOH, 90:10), **13** as a colorless oil (298 mg, 90%). The free base was converted to the hydrochloride and recrystallized from *i*-PrOH-Et_2O to give a white solid. M.p. (HCl) 157−159 °C; R_f (free base) 0.14 (CH_2Cl_2-MeOH, 95:5); ^{1}H NMR (400 MHz, $CDCl_3$, free base): δ 7.69−7.71 (m, 1H), 7.45 (s, 1H), 7.34−7.36 (m, 1H), 7.24−7.28 (m, 1H), 7.18−7.23 (m, 1H), 4.42 (dt, $^2J_{HF}$ = 47.6 Hz, $^3J_{HH}$ = 6.0 Hz, 2H, CH_2F), 4.15 (t, J = 7.2 Hz, 2H, NCH_2), 3.74 (t, J = 4.8 Hz, 4H, 2 × CH_2), 2.45 (t, J = 4.8 Hz, 4H, 2 × CH_2), 2.33 (s, 3H, NCH_3), 1.92 (quin., J = 7.2 Hz, 2H, CH_2), 1.67−1.77 (m, 2H, CH_2), 1.43−1.51 (m, 2H, CH_2); ^{13}C NMR (100 MHz, $CDCl_3$, free base): δ 166.7 (CO), 135.9 (quat.), 130.7 (CH), 126.3 (quat.), 122.5 (CH), 121.0 (CH), 120.9 (CH), 110.8 (quat.), 110.0 (CH), 83.8 (d, $^1J_{CF}$ = 164.0 Hz, CH_2F), 55.5 (2 × NCH_2), 46.7 (NCH_2), 46.3 (NCH_3), 45.2 (2 × NCH_2), 30.1 (d, $^2J_{CF}$ = 20.0 Hz, CH_2), 29.9 (CH_3), 23.0 (d, $^3J_{CF}$ = 5.0 Hz, CH_2); HRMS (ESI) $C_{19}H_{26}FN_3O$ exact mass 331.2060, accurate mass 331.2063 (mass error 0.93 ppm).

*(4-Ethylpiperazin-1-yl)(1-(5-fluoropentyl)-1H-indol-3-yl)-methanone Hydrochloride (**14**·HCl).* Subjecting **12** (317 mg, 1.00 mmol) and acetaldehyde (56 μL, 1.00 mmol, 1.0 equiv) to the general procedure gave, following purification by flash chromatography (CH_2Cl_2-MeOH, 90:10), **14** as a colorless oil (324 mg, 94%). The free base was converted to the hydrochloride and recrystallized from *i*-PrOH-Et_2O to give a white solid. M.p. (HCl) 175−177 °C; R_f (free base) 0.17 (CH_2Cl_2-MeOH, 95:5); ^{1}H NMR (400 MHz. $CDCl_3$, free base): δ 7.69−7.71 (m, 1H), 7.44 (s, 1H), 7.33−7.36 (m, 1H), 7.17−7.27 (m, 2H), 4.41 (dt, $^2J_{HF}$ = 47.2 Hz, $^3J_{HH}$ = 6.0 Hz, 2H, CH_2F), 4.14 (t, J = 7.2 Hz, 2H, NCH_2), 3.75 (t, J = 4.8 Hz, 4H, 2 × NCH_2), 2.43−2.50 (m, 6H, 2 × NCH_2 and 1 × CH_2), 1.91 (quin., J = 7.2 Hz, 2H, CH_2), 1.64−1.76 (m, 2H, CH_2), 1.42−1.50 (m, 2H, CH_2), 1.10 (t, J = 7.2 Hz, 3H, CH_3); ^{13}C NMR (free base, $CDCl_3$, 100 MHz): δ 166.6 (CO), 135.8 (quat.), 130.6 (CH), 126.3 (quat.), 122.4 (CH), 120.92 (CH), 120.87 (CH), 110.7 (quat.), 110.0 (CH), 83.8 (d, $^1J_{CF}$ = 164.0 Hz, CH_2F), 53.2 (2 × NCH_2), 52.4 (NCH_2), 46.7 (NCH_2), 45.4 (2 × CH_2), 30.0 (d, $^2J_{CF}$ = 20.0 Hz, CH_2), 29.8 (CH_2), 23.0 (d, $^3J_{CF}$ = 5.0 Hz, CH_2), 12.1 (CH_3); HRMS (ESI) $C_{20}H_{28}FN_3O$ exact mass 345.2216, accurate mass 345.2217 (mass error 0.17 ppm).

*(4-Propylpiperazin-1-yl)(1-(5-fluoropentyl)-1H-indol-3-yl)-methanone Hydrochloride (**15**·HCl).* Subjecting **12** (317 mg, 1.00 mmol) and propanal (72 μL, 1.00 mmol, 1.0 equiv) to the general procedure gave, following purification by flash chromatography (CH_2Cl_2-MeOH, 95:5), **15** as a colorless oil (342 mg, 95%). The free base was converted to the hydrochloride and recrystallized from EtOAc to give a white solid. M.p. (HCl) 105−108 °C; R_f (free base) 0.29 (CH_2Cl_2-MeOH, 95:5); ^{1}H NMR (400 MHz, $CDCl_3$, free base): δ 7.69−7.71 (m, 1H), 7.44 (s, 1H), 7.34−7.36 (m, 1H), 7.18−7.28 (m, 2H), 4.42 (dt, $^2J_{HF}$ = 47.2 Hz, $^3J_{HH}$ = 6.0 Hz, 2H, CH_2F), 4.14 (t, J = 7.2 Hz, 2H, NCH_2), 3.74 (t, J = 4.8 Hz, 4H, 2 × NCH_2), 2.48 (t, J = 4.8 Hz, 4H, 2 × NCH_2), 2.32−2.36 (m, 2H, CH_2), 1.91 (quin., J = 7.2 Hz, 2H, CH_2), 1.66−1.77 (m, 2H, CH_2), 1.43−1.57 (m, 4H, 2 × CH_2), 0.91 (t, J = 7.2 Hz, 3H, CH_3); ^{13}C NMR (free base, $CDCl_3$, 100 MHz): δ 166.6 (CO), 135.9 (quat.), 130.6 (CH), 126.3 (quat.), 122.4 (CH), 120.94, (CH), 120.91 (CH), 110.8 (quat.), 110.0 (CH), 83.8 (d, $^1J_{CF}$ = 164.0 Hz, CH_2F), 60.7 (NCH_2), 53.6 (2 × NCH_2), 46.7 (NCH_2), 45.3 (2 × NCH_2), 30.1 (d, $^2J_{CF}$ = 19.0 Hz, CH_2), 29.9 (CH_2), 23.0 (d, $^3J_{CF}$ = 5.0 Hz, CH_2), 20.1 (CH_2), 12.0 (CH_3); HRMS (ESI) $C_{21}H_{30}FN_3O$ exact mass 359.2373, accurate mass 359.2375 (mass error 0.46 ppm).

*(4-Benzylpiperazin-1-yl)(1-(5-fluoropentyl)-1H-indol-3-yl)-methanone Hydrochloride (**16**·HCl).* Subjecting **12** (317 mg, 1.00 mmol) and benzaldehyde (102 μL, 1.00 mmol, 1.0 equiv) to the general procedure gave, following purification by flash chromatography (CH_2Cl_2-MeOH, 95:5), **16** as a colorless oil (383 mg, 94%). The free base was converted to the hydrochloride and recrystallized from MeOH-Et_2O to give a white solid. M.p. (HCl) 199−201 °C; R_f (free base) 0.34 (CH_2Cl_2-MeOH, 95:5); ^{1}H NMR (400 MHz, $CDCl_3$, free base): δ 7.69−7.72 (m, 1H), 7.44 (s, 1H), 7.30−7.36 (m, 5H), 7.17−7.28 (m, 3H), 4.42 (dt, $^2J_{HF}$ = 47.6 Hz, CH_2F, 2H), 4.14 (t, J = 7.2 Hz, 2H, NCH_2), 3.74 (t, J = 4.8 Hz, 4H, 2 × NCH_2), 3.55 (s, 2H, C$\underline{H}_2$Ph), 2.50 (t, J = 4.8 Hz, 4H, 2 × NCH_2), 1.91 (quin., J = 7.6 Hz, 2H, CH_2), 1.65−1.78 (m, 2H, CH_2), 1.43−1.51 (m, 2H, CH_2); ^{13}C NMR (100 MHz, $CDCl_3$, free base): δ 166.7 (CO), 137.9 (quat.), 135.9 (quat.), 130.6 (CH), 129.3 (2 × CH), 128.4 (2 × CH_2), 127.3 (CH), 126.3 (quat.), 122.4 (CH), 120.9 (CH), 110.8 (quat.), 110.0 (CH), 83.8 (d, $^1J_{CF}$ = 164.0 Hz, CH_2F), 63.1 ($\underline{C}H_2$Ph), 53.5 (2 × NCH_2), 46.7 (NCH_2), 45.5 (2 × NCH_2), 30.1 (d, $^2J_{CF}$ = 19.0 Hz, CH_2), 29.85 (CH_2), 23.0 (d, $^3J_{CF}$ = 5.0 Hz, CH_2); HRMS (ESI) $C_{25}H_{30}FN_3O$ exact mass 407.2373, accurate mass 407.2374 (mass error 0.20 ppm).

*Synthesis of (Piperazin-1-yl)(1-alkyl-1H-indol-3-yl)methanone Hydrochlorides (**6**·HCl and **12**·HCl). (Piperazin-1-yl)(1-pentyl-1H-indol-3-yl)methanone Hydrochloride (**6**·HCl).* *tert*-Butyl 4-(1-pentyl-1*H*-indole-3-carbonyl)piperazine-1-carboxylate (**11**, 639 mg, 1.6 mmol) was dissolved in 1,4-dioxane (12 mL) and added dropwise to a cooled (0 °C) solution of 4 M hydrogen chloride in 1,4-dioxane (4 mL, 16 mmol, 10 equiv). The solution was stirred for 16 h, and the reaction mixture was evaporated under reduced pressure to afford the crude hydrochloride salt, which was washed with ice-cold anhydrous Et_2O (3 × 10 mL) and recrystallized from MeOH-Et_2O to afford **6·HCl** as a white solid (489 mg, 91%). M.p. (HCl) 161−163 °C; ^{1}H NMR (400 MHz, $CDCl_3$, free base): δ 7.68−7.70 (m, 1H), 7.45 (s, 1H), 7.34−7.37 (m, 1H), 7.17−2.27 (m, 2H), 4.12 (t, J = 7.2 Hz, 2H, NCH_2), 3.71 (t, J = 4.8 Hz, 4H, 2 × CH_2), 2.91 (t, J = 4.8 Hz, 4H, 2 × CH_2), 1.86 (quin., J = 7.2 Hz, 2H, CH_2), 1.28−1.39 (m, 4H, 2 × CH_2), 0.89 (t, J = 7.2 Hz, 3H, CH_3); ^{13}C NMR (100 MHz, $CDCl_3$, free base): δ 166.9 (CO), 135.9 (quat.), 130.7 (CH), 126.2 (quat.), 122.4 (CH), 120.9 (CH), 120.8 (CH), 110.5 (quat.), 110.1 (CH), 46.9 (NCH_2), 46.5(2) (2 × NCH_2), 46.5(0) (br overlapping, 2 × NCH_2) 29.9, (CH_2), 29.2 (CH_2), 22.4 (CH_2), 14.1 (CH_3); HRMS (ESI) $C_{18}H_{25}N_3O$ exact mass 299.1998, accurate mass 299.2001 (mass error 0.98 ppm).

*(Piperazin-1-yl)(1-(5-fluoropentyl)-1H-indol-3-yl)methanone Hydrochloride (**12**·HCl).* Subjecting *tert*-butyl 4-(1-(5-fluoropentyl)-1*H*-

indole-3-carbonyl)piperazine-1-carboxylate (**17**, 668 mg, 1.6 mmol) to the procedure described for **6·HCl** gave **12·HCl**, which was recrystallized from MeOH-Et_2O to furnish a white solid (476 mg, 84%). M.p. (HCl) 139−142 °C; ^{1}H NMR (400 MHz, $CDCl_3$, free base): δ 7.67−7.70 (m, 1H), 7.46 (s, 1H), 7.34−7.36 (m, 1H), 7.28−7.18 (m, 2H), 4.42 (dt, $^2J_{HF}$ = 47.2 Hz, $^3J_{HH}$ = 6.0 Hz, 2H, CH_2F), 4.15 (t, J = 7.2 Hz, 2H, NCH_2), 3.72 (t, J = 5.2 Hz, 4H, 2 × NCH_2), 2.93 (t, J = 5.2 Hz, 4H, 2 × NCH_2), 1.92 (quin., J = 7.6 Hz, 2H, CH_2), 1.65−1.78 (m, 2H, 2 × CH_2), 1.43−1.51 (m, 2H, 2 × CH_2); ^{13}C NMR (100 MHz, $CDCl_3$, free base): δ 166.9 (CO), 135.9 (quat.), 130.7 (CH), 126.2 (quat.), 122.5 (CH), 121.0 (CH), 120.8 (CH), 110.6 (quat.), 110.0 (CH), 83.8 (s,$^1J_{CF}$ = 164.0 Hz, CH_2F), 46.7 (NCH_2), 46.3 (2 × NCH_2), 46.2 (br overlapping, 2 × NCH_2), 30.1 (d, $^2J_{CF}$ = 20.0 Hz, CH_2), 29.8 (CH_3), 23.0 (d, $^3J_{CF}$ = 5.0 Hz, CH_2); HRMS (ESI) $C_{18}H_{24}FN_3O$ exact mass 317.1903, accurate mass 317.1908 (mass error 1.32 ppm).

*Synthesis of tert-Butyl 4-(1-Alkyl-1H-indole-3-carbonyl)-piperazine-1-carboxylates (**11** and **17**). tert-Butyl 4-(1-Pentyl-1H-indole-3-carbonyl)piperazine-1-carboxylate (**11**).* To a solution of 1-pentyl-1*H*-indole-3-carboxylic acid (**23**, 463 mg, 2.0 mmol) in DMF (10 mL) was added HOBt·H_2O (337 mg, 2.2 mmol, 1.1 equiv), EDC·HCl (498 mg, 2.6 mmol, 1.3 equiv), 1-Boc-piperazine (373 mg, 2.0 mmol, 1.0 equiv), and Et_3N (833 μL, 6.0 mmol, 3.0 equiv), and the mixture was stirred at ambient temperature for 14 h. The mixture was poured onto H_2O (400 mL) and extracted with EtOAc (3 × 100 mL), and the combined organic phases were washed with H_2O (2 × 100 mL) and brine (100 mL), dried ($MgSO_4$), and the solvent was evaporated under reduced pressure. The crude material was purified using flash chromatography (CH_2Cl_2-MeOH, 98:2) to give **11** as a colorless solid (734 mg, 92%). M.p. 82−84 °C; R_f 0.38 (CH_2Cl_2-MeOH, 95:5); ^{1}H NMR (400 MHz, $CDCl_3$): δ 7.68 (d, J = 7.4 Hz, 1H), 7.47 (s, 1H), 7.37 (d, J = 7.9 Hz, 1H), 7.17−7.29 (m, 2H), 4.12 (t, J = 7.2 Hz, 2H, NCH_2), 3.63−3.75 (m, 4H, 2 × NCH_2), 3.45−3.55 (m, 4H, 2 × NCH_2), 1.87 (quin., J = 7.2 Hz, 2H, CH_2), 1.47 (s, 9H, 3 × CH_3), 1.28−1.41 (m, 4H, 2 × CH_2), 0.89 (t, J = 6.8 Hz, 3H, CH_3); ^{13}C NMR (100 MHz, $CDCl_3$): δ 167.1 (CO), 154.9 (N$\underline{C}O_2t$Bu), 135.9 (quat.), 130.9 (CH), 126.1 (quat), 122.5 (CH), 121.0 (CH), 120.7 (CH), 110.6 (CH), 110.1 (quat.), 80.3 (quat.), 46.9 (NCH_2), 45.4 (br, 2 × NCH_2), 44.0 (br, 2 × NCH_2), 29.8 (CH_2), 29.2 (CH_2), 28.5 (3 × CH_3), 22.4 (CH_2), 14.0 (CH_3); HRMS (ESI) $C_{23}H_{33}N_3O_3$ exact mass 399.2522, accurate mass 399.2523 (mass error 0.23 ppm).

*tert-Butyl 4-(1-(5-Fluoropentyl)-1H-indole-3-carbonyl)-piperazine-1-carboxylate (**17**).* Subjecting 1-(5-fluoropentyl)-1*H*-indole-3-carboxylic acid (**24**, 463 mg, 2.0 mmol) to the procedure described for **11** afforded, following purification by flash chromatography (CH_2Cl_2-MeOH, 95:5), **17** as a colorless resin (741 mg, 89%). R_f 0.29 (CH_2Cl_2-MeOH, 95:5); ^{1}H NMR (400 MHz, $CDCl_3$): δ 7.68 (d, J = 7.5 Hz, 1H), 7.46 (s, 1H), 7.36 (d, 1H), 7.17−7.30 (m, 2H), 4.43 (dt, $^2J_{HF}$ = 47.3, $^3J_{HH}$ = 5.9 Hz, 2H, CH_2F), 4.16 (t, J = 7.2 Hz, 2H, NCH_2), 3.63−3.75 (m, 4H, 2 × NCH_2), 3.46−3.53 (m, 4H, 2 × NCH_2), 1.92 (quin., J = 7.2 Hz, 2H, CH_2), 1.63−1.83 (m, 2H, CH_2), 1.47 (s overlapping, 9H, 3 × CH_3), 1.44−1.53 (m overlapping, 2H, CH_2); ^{13}C NMR (100 MHz, $CDCl_3$): δ 167.0 (CO), 154.8 (N$\underline{C}O_2t$Bu), 135.9 (quat.), 130.8 (CH), 126.2 (quat.), 122.6 (CH), 121.1 (CH), 120.8(CH), 110.4 (quat.), 110.1 (CH), 83.76 (d, $^1J_{CF}$ = 165.0 Hz, CH_2), 80.3 (quat.), 46.7 (NCH_2), 45.3 (br, 2 × NCH_2), 44.6 (br, 2 × NCH_2), 30.7 (d, $^2J_{CF}$ = 19.8 Hz, CH_2), 29.8 (CH_2), 28.5 (3 × CH_3), 23.0 (d, $^2J_{CF}$ = 4.9 Hz, CH_2); HRMS (ESI) $C_{23}H_{32}FN_3O_3$ exact mass 417.2428, accurate mass 417.2433 (mass error 1.28 ppm).

*General Procedure for Synthesis of 1-Alkyl-1H-indole-3-carboxylic Acids (**23** and **24**).* To a cooled (0 °C) suspension of sodium hydride (60% dispersion in mineral oil, 1.20 g, 30.0 mmol, 2.0 equiv) in DMF (15 mL) was added dropwise a solution of indole (1.76 g, 15.0 mmol) in DMF (2 mL) and the mixture was allowed to stir at ambient temperature for 10 min. The mixture was cooled (0 °C), treated dropwise with the appropriate alkyl bromide (15.8 mmol, 1.05 equiv), and stirred at ambient temperature for 1 h. The mixture was cooled (0 °C), treated portionwise with trifluoroacetic anhydride (5.20 mL, 37.5 mmol, 2.5 equiv), and stirred at ambient temperature for 1 h. The solution was poured portionwise onto vigorously stirred ice water (900 mL) until precipitation was complete, and the formed red-pink solid was filtered and air-dried overnight.

To a refluxing solution of potassium hydroxide (2.78 g, 49.5 mmol, 3.3 equiv) in methanol (5 mL) was added portionwise a solution of the crude 1-alkyl-3-trifluoroacetyl-1*H*-indole in toluene (15 mL) and the solution was heated at reflux for 2 h. The solution was cooled to ambient temperature and partitioned between 1 M aq. NaOH (400 mL) and Et_2O (50 mL). The layers were separated, and the aqueous layer was adjusted to pH 1 with 10 M aq. HCl. The aqueous phase was extracted with Et_2O (3 × 100 mL), dried (Na_2SO_4), and solvent-evaporated under reduced pressure. The crude product was recrystallized from *i*-PrOH.

*1-Pentyl-1H-indole-3-carboxylic Acid (**23**).* Subjecting 1-bromopentane (1.95 mL, 15.8 mmol) to the general procedure above gave **23** as a colorless crystalline solid (1.92 g, 55% over two steps). ^{1}H NMR (400 MHz, $CDCl_3$): δ 8.24−8.27 (m, 1H), 7.93 (s, 1H), 7.38−7.40 (m, 1H), 7.29−7.33 (m, 2H), 4.17 (t, 2H, J = 7.2 Hz, NCH_2), 1.90 (quin, 2H, J = 7.2 Hz, CH_2), 1.32−1.39 (m, 4H, 2 × CH_2), 0.91 (t, 3H, J = 7.0 Hz, CH_3). All physical and spectral properties matched those reported previously.[58]

*1-(5-Fluoropentyl)-1H-indole-3-carboxylic Acid (**24**).* Subjecting 1-bromo-5-fluoropentane (0.195 mL, 1.58 mmol) to the general procedure gave **23** as a colorless crystalline solid (0.249 g, 67% over two steps). ^{1}H NMR (400 MHz, $CDCl_3$): δ 8.21−8.29 (m, 1H, CH), 7.93 (s, 1H, CH), 7.36−7.42 (m, 1H, CH), 7.29−7.34 (m, 2H, CH), 4.43 (dt, $^2J_{CF}$ = 47.2, $^3J_{HH}$ = 5.9 Hz, 2H, CH_2F), 4.20 (t, J = 7.1 Hz, 2H, NCH_2), 1.96 (quin., J = 7.3 Hz, 2H, CH_2), 1.65−1.83 (m, 2H, CH_2), 1.43−1.53 (m, 2H, CH_2). All physical and spectral properties matched those reported previously.[12]

***In Vitro* CB_1 and CB_2 Binding Experiments.** Receptor affinity was determined as previously described.[11] Membranes containing either triple-hemagglutinated, human CB_1 with preprolactin signal sequence, 3HA-hCB1[65] or CB_2 3HA-hCB2,[66] were isolated from HEK293 cells (ATCC #CRL-1573, Manassas, VA) stably expressing each receptor (both in pEF4a). Cells were cultivated until semiconfluent in 175 cm^2 polystyrene culture flasks in Dulbecco's modified Eagle's medium supplemented with 10% fetal bovine serum (FBS, *v*/*v*, ThermoFisher Scientific, Waltham MA) and 250 μg/ml zeocin. Cells were suspended with 5 mM ice-cold EDTA in phosphate-buffered saline (PBS) and pelleted at 200*g* for 5 min. The supernatant was discarded, and the pellet was snap-frozen at −80 °C. To purify membranes, pellets were thawed on ice with tris−sucrose buffer (50 mM tris−HCl pH 7.4, 200 mM sucrose, 5 mM $MgCl_2$, 2.5 mM EDTA) and homogenized manually using a glass homogenizer. The homogenate was centrifuged at 1000*g* for 10 min at 4 °C. The supernatant was retained and further centrifuged at 27,000 rcf for 30 min at 4 °C. The pellet was suspended in a minimal volume of tris−sucrose buffer, aliquoted and stored at −80 °C. The protein concentration was quantified using a DC protein assay (Bio-Rad, Hercules, CA) adhering to the manufacturer's protocol.

CB_1- or CB_2-containing membranes (7.5 μg/point) were, respectively, incubated with 1 nM radioactively labeled [^{3}H]-SR141716A (specific activity 55 Ci/mmol, PerkinElmer, Waltham MA) or [^{3}H]CP 55,940 (specific activity 175 Ci/mmol, PerkinElmer) and either 10 μM (preliminary screen) or a range from 0.1 nM of 10 μM (for K_i determination) of the unlabeled test compound for 1 h at 30 °C. All components were diluted to a final assay volume of 200 μL in binding buffer (50 mM HEPES pH 7.4, 1 mM $MgCl_2$, 1 mM $CaCl_2$, 0.2% *w*/*v* bovine serum albumin (BSA, MP Biomedicals, Auckland, NZ)). Harvest plates (96-well GF/C, PerkinElmer) were simultaneously soaked for 1 h at room temperature in 0.1% (*w*/*v*) branched polyethyleneimine (Sigma-Aldrich) in H_2O. Harvest plates were applied to a vacuum manifold (Pall Corp., New York, NY) at 5−10 mmHg and washed with 200 μL wash buffer (50 mM HEPES pH 7.4, 500 mM NaCl, 0.1% (*w*/*v*) BSA). Test solutions were filtered through and thrice washed with 200 μL wash buffer. Harvest plates were dried overnight at room temperature. After sealing the base of the plate with a clear plate sealer, scintillation fluid (IRGASAFE Plus, PerkinElmer) was applied to each well (50 μL/well) and incubated in dark conditions for 30 min prior to detection using a Wallac TriLux MicroBeta2 scintillation counter for 2 min/well (PerkinElmer). Data were exported

https://doi.org/10.1021/acschemneuro.1c00822
ACS Chem. Neurosci. 2022, 13, 1395−1409

and analyzed in GraphPad PRISM (version 8.0., GraphPad Software Inc. San Diego, CA) and expressed as receptor affinity (pK_i), and the maximum displacement of the reference compound (%) from at least three individual experiments was performed in duplicate. Receptor affinity was estimated using a "one-site fit K_i" model, with radioligand K_d previously determined to be 1 nM (for both [^{3}H]SR141716A and [^{3}H]CP 55,940 for CB_1 and CB_2, respectively).

***In Vitro* CB_1 and CB_2 and $Ca_V3.x$ Functional Activity Experiments.** *Transfection and Cell Culture.* All $Ca_V3.x$ experiments were performed using HEK293 FlpIn T-Rex cells stably transfected with pcDNA5 constructs encoding human $Ca_V3.x$ cDNA.[63] $Ca_V3.x$ expression was induced 24 h before membrane potential assays or electrophysiology experiments by adding 2 μg/mL tetracycline. Human CB_1 or CB_2 was stably transfected into AtT-20 FlpIn and maintained using 80 μg/mL hygromycin within the culture media. Cells were maintained and passaged at an 80% confluency in 75 cm^2 flasks and kept at 37 °C/5% CO_2 and used for up to 30 passages. Cells for calcium flux and membrane potential assays were grown in the same conditions but used at >90% confluence.

Functional Assays. Changes in membrane potential and calcium flux of cells were measured using the FLIPR membrane potential assay (MPA) or calcium 5 assay (Ca5) kits (Molecular Devices, Sunnyvale, CA), as previously described.[53,67] Briefly, 24 h prior to the assay, AtT-20-CB_1/CB_2 or HEK293-$Ca_V3.x$ cells were detached from their flasks using trypsin/EDTA (Sigma-Aldrich) and resuspended in 10 mL Leibovitz's L-15 media supplemented with 1% FBS, 100 μg penicillin and streptomycin per mL, and 15 mM glucose (and 2 μg/mL tetracycline for HEK293-$Ca_V3.x$). Cells were plated in a volume of 90 μL per well in black-walled, clear-bottomed 96-well microplates (Corning, Castle Hill, Australia) and incubated overnight at 37 °C in ambient CO_2. MPA or Ca5 dye was reconstituted with the assay buffer (HBSS) containing the following compounds in mM: NaCl 145, HEPES 22, Na_2HPO4 0.338, $NaHCO_3$ 4.17, KH_2PO_4 0.441, $MgSO_4$ 0.407, $MgCl_2$ 0.493, $CaCl_2$ 1.26, and glucose 5.56, pH 7.4, osmolarity 315 mOSM at half the manufacturer's recommended concentration. For Ca5 experiments, the HBSS was supplemented with probenecid (2.5 mM, Biotium, Scoresby, VIC, Australia) to minimize dye loss from the cells. Cells were loaded with 90 μL per well of the dye solution without removal of the L-15 and incubated at 37 °C for 60 min in ambient CO_2. Fluorescence was measured using a FlexStation 3 microplate reader (Molecular Devices, λ_{ex} 530 nm/λ_{em} 565 nm for MPA or λ_{ex} 485 nm/λ_{em} 525 nm for Ca5) using SoftMax Pro 7 (Molecular Devices). Baseline readings were taken every 2 s for at least 2 min, at which time the diluted drug was added in a volume of 20 μL. For the MPA assay of CB_1/CB_2 activity, changes in fluorescence elicited by the addition of drug were expressed as a percentage of baseline fluorescence after subtraction of the changes produced by vehicle addition, normalized to the maximal effective response elicited from 1 μM CP 55,940 within each column, as previously described.[67] For measuring the modulation of $Ca_V3.x$ activity, $CaCl_2$ was added to cells (final concentration 10 mM) 5 min after the drug and the changes in Ca5 fluorescence were expressed as a change relative to 10 mM Ca alone (area under the curve). The final concentration of the vehicle (dimethyl sulfoxide (DMSO)) was not more than 0.1% in both assays, and Ca^{2+} and K^+ concentrations in the CaV assay buffer solution were approximately 10 and 2.5 mM, respectively. Data from both assays were analyzed with Graphpad PRISM and are expressed as the mean ± SEM of at least five independent determinations performed in duplicate unless otherwise stated.

Electrophysiology. Whole-cell voltage-clamp recordings from HEK293-$Ca_V3.x$ cells were performed at room temperature. At least 24 h prior to experiments, cells were detached from flasks using trypsin/EDTA and plated into 10 cm sterile tissue culture dishes containing 10 mL of supplemented DMEM and 10−15 glass coverslips (12 mm diameter, ProScitech, QLD, Australia). Culture dishes were then kept overnight in the same conditions as flasks to allow cells to adhere to coverslips. They were then transferred to a 30 °C/5% CO_2 incubator to inhibit cell proliferation until ready to be used for electrophysiology experiments.

Recording Solutions. External recording solutions contained (in mM) 114 CsCl, 5 $BaCl_2$, 1 $MgCl_2$, 10 HEPES, 10 glucose, adjusted to pH 7.4 with CsOH. The internal patch pipette solution contained (in mM) 126.5 $CsMeSO_4$, 2 $MgCl_2$, 11 EGTA, and 10 HEPES adjusted to pH 7.3 with CsOH. The internal solution was supplemented with 0.6 mM GTP and 2 mM ATP and mixed thoroughly just prior to use. Liquid junction potentials for the above solutions were calculated prior to experiments using pClamp 10 software and corrected for during experiments. Compounds were prepared daily from 10 mM DMSO stocks and diluted into the external solution just prior to use. Compounds were then applied rapidly and locally to the cells using a custom-built gravity-driven microperfusion system.[68] Initial vehicle experiments were performed to ensure that 0.1% DMSO had no effect on current amplitudes or channel kinetics (data not shown), and all subsequent experiments contained 0.1% DMSO in control external solutions. Currents were elicited from a holding potential of −100 mV and were measured by conventional whole-cell patch-clamp techniques using an Axopatch 200B amplifier in combination with Clampex 9.2 software (Molecular Devices, Sunnyvale). After establishing whole-cell configuration, the cellular capacitance was minimized using the amplifier's built-in analogue compensation. Series resistance was kept to <10 MΩ and was compensated to at least 85% in all experiments. All data were digitized at 10 kHz with a Digidata 1320 interface (Molecular Devices) and filtered at 1 kHz (8-pole Bessel filter). Raw and online leak-subtracted data were both collected simultaneously, and P/N4 leak subtraction was performed using opposite polarity and after the protocol sweep. For tonic inhibition of T-type current, membrane potential was stepped from −100 to −30 mV for 200 ms and then allowed to recover for 12 s (one sweep). A minimum of 10 sweeps were collected under control external perfusion to allow for control peak current to equilibrate. The drug was then continuously perfused, and sweeps were recorded until no further inhibition is seen (minimum of three sweeps with the same amplitude). All electrophysiology data were acquired and analyzed using Clampfit 9.2 (Molecular Devices) and are expressed as a percentage of means ± standard errors of at least six experiments per compound on each calcium channel.

***In Vivo* Radiobiotelemetry.** Radiobiotelemetric assessment of MEPIRAPIM and 5F-BEPIRAPIM was carried out according to previously reported procedures.[11,54,69] Briefly, TA-F10 radiobiotelemetry probes (Data Sciences International, St. Paul) were intraperitoneally implanted according to the manufacturer's instructions into male C57BL/6J mice. The mice were aged 8 weeks at the time of surgery, weighed between 20 and 25 g, and were allowed 10 days of recovery time before data collection. All work involving animals was carried out in accordance with the Australian Code of Practice for the Care and Use of Animals for Scientific Purposes and approved by The University of Sydney Animal Ethics Committee.

Four mice were used per drug, and the first received a "baseline" vehicle injection of a 5:5:90 mixture of ethanol, polysorbate 80, and saline, respectively. Mice then received an ascending dose sequence of 0.1, 0.3, 1, 3, 10, and 30 mg/kg, with two drug-free washout days between each dose to minimize the development of drug tolerance. The drugs were administered via intraperitoneal injection with an injection volume of 10 μL/g.

Raw body temperature data were gathered continuously at 1000 Hz and averaged into 15 min bins using Dataquest A.R.T. software (version 4.33, Data Sciences International). Using Prism (version 8.4.3), baseline (vehicle injection) data for each animal were subtracted to yield the change in body temperature data. Area under baseline curves (AUCs) for the first 2.5 h were calculated for each drug dose using R (version 4.0.5) as a measure of the total drug effect. For the 30 mg/kg MEPIRAPIM drug dose, the mean AUC was compared to zero (i.e., no change from baseline) using a one-sample t-test.

Molecular Docking Simulations. *Protein Preparation.* The cryo-EM structures of the CB1 receptor (PDB: 6N4B)[70] and CB2 receptor (PDB: 6TP0)[71] were retrieved from RCSB PDB (https://www.rcsb.org/). The structure was prepared using Protein Preparation Wizard.[72] The G proteins and cholesterol molecule were removed, leaving only the receptor and ligand in the active site. The preparation process involved assigning bond orders, adding hydrogens, creating zero-order

https://doi.org/10.1021/acschemneuro.1c00822
ACS Chem. Neurosci. 2022, 13, 1395−1409

bonds to metals, generating disulfide bonds, filling in missing side chains and loops using Prime, generating het states using Epik[73] at pH 7.0 ± 2.0, and deleting water molecules beyond 5 Å from het groups. The hydrogen bond network was optimized, and water orientations were sampled. The pK_a values of the protein were predicted using PROPKA,[74] and the target pH value was set at 7.0. Lastly, the protein structure was minimized using the OPLS_2005 force field[75] where the RMSD of the atom displacement for terminating the minimization was set as 0.3 Å.

Ligand Preparation. Ligands were first prepared using LigPrep[76] to generate energy-minimized three-dimensional (3D) structures. OPLS3e force field was used for minimization. Epik was used to generate all possible ionized states at pH 7.0 ± 2.0. The desalt setting was used to remove any counterions or water molecules. Tautomer and stereoisomers were generated (at most 32 per ligand), where specified chiralities were retained.

Induced Fit Docking. To generate docking poses, prepared ligands were docked against the prepared CB1 and CB2 structures using induced fit docking.[77] Extended sampling protocol and OPLS3e force field were used. The ligand in the binding site was used to define the receptor. The core constraint was applied to restrict docking to the ligand with a tolerance of 1.0 Å; core atoms were determined based on the maximum common structure. Ring conformation sampling was performed with an energy window set as 2.5 kcal/mol; nonplanar conformation was penalized for amide bonds. Residues within 5.0 Å of ligand poses were refined using Prime.

■ ASSOCIATED CONTENT

Supporting Information

The Supporting Information is available free of charge at https://pubs.acs.org/doi/10.1021/acschemneuro.1c00822.

^{1}H and ^{13}C NMR spectra for all novel compounds and representative fluorescence inhibition and electrophysiology traces for selected compounds at T-type calcium channels (PDF)

■ AUTHOR INFORMATION

Corresponding Author

Samuel D. Banister − *The Lambert Initiative for Cannabinoid Therapeutics, Brain and Mind Centre, The University of Sydney, NSW 2050, Australia; School of Chemistry, The University of Sydney, NSW 2006, Australia;* orcid.org/0000-0002-4690-4318; Phone: +61 2 9351 0805; Email: samuel.banister@sydney.edu.au

Authors

Richard C. Kevin − *The Lambert Initiative for Cannabinoid Therapeutics, Brain and Mind Centre, The University of Sydney, NSW 2050, Australia; School of Pharmacy, The University of Sydney, NSW 2006, Australia;* orcid.org/0000-0002-4912-4499

Somayeh Mirlohi − *Faculty of Medicine, Health and Human Sciences, Macquarie University, NSW 2109, Australia*

Jamie J. Manning − *Department of Pharmacology and Toxicology, University of Otago, Dunedin 9016, New Zealand*

Rochelle Boyd − *The Lambert Initiative for Cannabinoid Therapeutics, Brain and Mind Centre, The University of Sydney, NSW 2050, Australia; School of Chemistry, The University of Sydney, NSW 2006, Australia*

Elizabeth A. Cairns − *The Lambert Initiative for Cannabinoid Therapeutics, Brain and Mind Centre, The University of Sydney, NSW 2050, Australia; School of Psychology, The University of Sydney, NSW 2006, Australia*

Adam Ametovski − *The Lambert Initiative for Cannabinoid Therapeutics, Brain and Mind Centre, The University of Sydney, NSW 2050, Australia; School of Chemistry, The University of Sydney, NSW 2006, Australia*

Felcia Lai − *School of Pharmacy, The University of Sydney, NSW 2006, Australia*

Jia Lin Luo − *The Lambert Initiative for Cannabinoid Therapeutics, Brain and Mind Centre, The University of Sydney, NSW 2050, Australia; School of Psychology, The University of Sydney, NSW 2006, Australia*

William Jorgensen − *School of Chemistry, The University of Sydney, NSW 2006, Australia;* orcid.org/0000-0002-9990-6894

Ross Ellison − *Clinical Toxicology and Environmental Biomonitoring Laboratory, University of California, San Francisco, California 94143, United States*

Roy R. Gerona − *Clinical Toxicology and Environmental Biomonitoring Laboratory, University of California, San Francisco, California 94143, United States*

David E. Hibbs − *School of Pharmacy, The University of Sydney, NSW 2006, Australia;* orcid.org/0000-0002-2635-2990

Iain S. McGregor − *The Lambert Initiative for Cannabinoid Therapeutics, Brain and Mind Centre, The University of Sydney, NSW 2050, Australia; School of Psychology, The University of Sydney, NSW 2006, Australia*

Michelle Glass − *Department of Pharmacology and Toxicology, University of Otago, Dunedin 9016, New Zealand;* orcid.org/0000-0002-5997-6898

Mark Connor − *Faculty of Medicine, Health and Human Sciences, Macquarie University, NSW 2109, Australia;* orcid.org/0000-0003-2538-2001

Chris Bladen − *Faculty of Medicine, Health and Human Sciences, Macquarie University, NSW 2109, Australia; Department of Physiology and Pharmacology, Hotchkiss Brain Institute, Alberta Children's Hospital Research Institute, Cumming School of Medicine, University of Calgary, Calgary, AB T2N 1N4, Canada*

Gerald W. Zamponi − *Department of Physiology and Pharmacology, Hotchkiss Brain Institute, Alberta Children's Hospital Research Institute, Cumming School of Medicine, University of Calgary, Calgary, AB T2N 1N4, Canada;* orcid.org/0000-0002-0644-9066

Complete contact information is available at: https://pubs.acs.org/10.1021/acschemneuro.1c00822

Author Contributions

A.M., J.L.L., and W.J. synthesized and analytically characterized all compounds under the supervision of S.D.B. J.M. performed the *in vitro* binding assays under the supervision of M.G. R.B. performed the *in vitro* CB_1 and CB_2 receptor membrane potential assays, and S.M. performed the Ca_V calcium flux and electrophysiology assays, under the supervision of M.C. and C.B. R.C.K. performed radiobiotelemetry experiments under the supervision of I.S.M. R.E. conducted high-resolution mass spectrometry under the supervision of R.R.G. F.L. conducted molecular docking simulations under the supervision of D.E.H. R.C.K., M.G., M.C., C.B., and S.D.B. conceived the experiments, and R.C.K., E.A.C., A.A., C.B., G.W.Z., and S.D.B. wrote the manuscript. All authors reviewed and edited drafts of the manuscript and approved the final version.

Funding

R.C.K., R.B., S.M., E.A.C., A.A., J.L.L., I.S.M., and S.D.B. gratefully acknowledge support from The Lambert Initiative for

Cannabinoid Therapeutics, a philanthropic research program based at the Brain and Mind Centre, The University of Sydney. Research by R.C.K., E.A.C., A.A., J.L.L., and S.D.B. was partially supported by the National Health and Medical Research Council Project Grant 1161571 and a Brain and Mind Centre Research Development Grant from The University of Sydney. W.J. is supported by a National Health and Medical Research Council Peter Doherty Early Career Research Fellow. Research by J.M. and M.G. was supported by a contract from the Health Research Council of New Zealand.

Notes

The authors declare no competing financial interest.

All work involving animals was carried out in accordance with the Australian Code of Practice for the Care and Use of Animals for Scientific Purposes and approved by The University of Sydney Animal Ethics Committee.

■ ABBREVIATIONS

ANOVA, analysis of variance; CB_1, cannabinoid receptor 1; CB_2, cannabinoid receptor 2; EDC, 1-ethyl-3-(3-dimethylaminopropyl)carbodiimide; EMCDDA, European Centre for Drugs and Drug Addiction; FBS, fetal bovine serum; FLIPR, fluorometric imaging plate reader; GTPγS, guanosine 5′-*O*-[gamma-thio]triphosphate; HEK, human embryonic kidney; HOBt, 1-hydroxybenzotriazole; NMR, nuclear magnetic resonance; NPS, new psychoactive substances; QTOF-MS, quadrupole time-of-flight mass spectrometry; SAR, structure−activity relationship; SCRA, synthetic cannabinoid receptor agonist; SEM, standard error of mean; THC, Δ^9-tetrahydrocannabinol

■ REFERENCES

(1) Banister, S. D.; Moir, M.; Stuart, J.; Kevin, R. C.; Wood, K. E.; Longworth, M.; Wilkinson, S. M.; Beinat, C.; Buchanan, A. S.; Glass, M.; Connor, M.; McGregor, I. S.; Kassiou, M. Pharmacology of Indole and Indazole Synthetic Cannabinoid Designer Drugs AB-FUBINACA, ADB-FUBINACA, AB-PINACA, ADB-PINACA, 5F-AB-PINACA, 5F-ADB-PINACA, ADBICA, and 5F-ADBICA. *ACS Chem. Neurosci.* **2015**, *6*, 1546−1559.

(2) Antonides, L. H.; Cannaert, A.; Norman, C.; NicDáeid, N.; Sutcliffe, O. B.; Stove, C. P.; McKenzie, C. Shape matters: The application of activity-based in vitro bioassays and chiral profiling to the pharmacological evaluation of synthetic cannabinoid receptor agonists in drug-infused papers seized in prisons. *Drug Test. Anal.* **2021**, *13*, 628−643.

(3) Banister, S. D.; Longworth, M.; Kevin, R.; Sachdev, S.; Santiago, M.; Stuart, J.; Mack, J. B.; Glass, M.; McGregor, I. S.; Connor, M.; Kassiou, M. Pharmacology of Valinate and tert-Leucinate Synthetic Cannabinoids 5F-AMBICA, 5F-AMB, 5F-ADB, AMB-FUBINACA, MDMB-FUBINACA, MDMB-CHMICA, and Their Analogues. *ACS Chem. Neurosci.* **2016**, *7*, 1241−1254.

(4) Banister, S. D.; Connor, M. The Chemistry and Pharmacology of Synthetic Cannabinoid Receptor Agonist New Psychoactive Substances: Evolution. *Handb. Exp. Pharmacol.* **2018**, *252*, 191−226.

(5) Cannaert, A.; Storme, J.; Franz, F.; Auwarter, V.; Stove, C. P. Detection and Activity Profiling of Synthetic Cannabinoids and Their Metabolites with a Newly Developed Bioassay. *Anal. Chem.* **2016**, *88*, 11476−11485.

(6) Angerer, V.; Bisel, P.; Moosmann, B.; Westphal, F.; Auwarter, V. Separation and structural characterization of the new synthetic cannabinoid JWH-018 cyclohexyl methyl derivative "NE-CHMIMO" using flash chromatography, GC-MS, IR and NMR spectroscopy. *Forensic Sci. Int.* **2016**, *266*, e93−e98.

(7) Franz, F.; Angerer, V.; Brandt, S. D.; McLaughlin, G.; Kavanagh, P. V.; Moosmann, B.; Auwarter, V. In vitro metabolism of the synthetic cannabinoid 3,5-AB-CHMFUPPYCA and its 5,3-regioisomer and investigation of their thermal stability. *Drug Test. Anal.* **2017**, *9*, 311−316.

(8) Mogler, L.; Franz, F.; Rentsch, D.; Angerer, V.; Weinfurtner, G.; Longworth, M.; Banister, S. D.; Kassiou, M.; Moosmann, B.; Auwarter, V. Detection of the recently emerged synthetic cannabinoid 5F-MDMB-PICA in 'legal high' products and human urine samples. *Drug Test. Anal.* **2018**, *10*, 196−205.

(9) Angerer, V.; Mogler, L.; Steitz, J. P.; Bisel, P.; Hess, C.; Schoeder, C. T.; Muller, C. E.; Huppertz, L. M.; Westphal, F.; Schaper, J.; Auwarter, V. Structural characterization and pharmacological evaluation of the new synthetic cannabinoid CUMYL-PEGACLONE. *Drug Test. Anal.* **2018**, *10*, 597−603.

(10) Schoeder, C. T.; Hess, C.; Madea, B.; Meiler, J.; Muller, C. E. Pharmacological evaluation of new constituents of "Spice": synthetic cannabinoids based on indole, indazole, benzimidazole and carbazole scaffolds. *Forensic Toxicol.* **2018**, *36*, 385−403.

(11) Banister, S. D.; Adams, A.; Kevin, R. C.; Macdonald, C.; Glass, M.; Boyd, R.; Connor, M.; McGregor, I. S.; Havel, C. M.; Bright, S. J.; Vilamala, M. V.; Lladanosa, C. G.; Barratt, M. J.; Gerona, R. R. Synthesis and pharmacology of new psychoactive substance 5F-CUMYL-P7AICA, a scaffold- hopping analog of synthetic cannabinoid receptor agonists 5F-CUMYL-PICA and 5F-CUMYL-PINACA. *Drug Test. Anal.* **2019**, *11*, 279−291.

(12) Banister, S. D.; Stuart, J.; Kevin, R. C.; Edington, A.; Longworth, M.; Wilkinson, S. M.; Beinat, C.; Buchanan, A. S.; Hibbs, D. E.; Glass, M.; Connor, M.; McGregor, I. S.; Kassiou, M. Effects of bioisosteric fluorine in synthetic cannabinoid designer drugs JWH-018, AM-2201, UR-144, XLR-11, PB-22, 5F-PB-22, APICA, and STS-135. *ACS Chem. Neurosci.* **2015**, *6*, 1445−1458.

(13) Uchiyama, N.; Kawamura, M.; Kikura-Hanajiri, R.; Goda, Y. Identification of two new-type synthetic cannabinoids, N-(1-adamantyl)-1-pentyl-1H-indole-3-carboxamide (APICA) and N-(1-adamantyl)-1-pentyl-1H-indazole-3-carboxamide (APINACA), and detection of five synthetic cannabinoids, AM-1220, AM-2233, AM-1241, CB-13 (CRA-13), and AM-1248, as designer drugs in illegal products. *Forensic Toxicol.* **2012**, *30*, 114−125.

(14) Trecki, J.; Gerona, R. R.; Schwartz, M. D. Synthetic Cannabinoid-Related Illnesses and Deaths. *N. Engl. J. Med.* **2015**, *373*, 103−107.

(15) Schwartz, M. D.; Trecki, J.; Edison, L. A.; Steck, A. R.; Arnold, J. K.; Gerona, R. R. A Common Source Outbreak of Severe Delirium Associated with Exposure to the Novel Synthetic Cannabinoid ADB-PINACA. *J. Emerg. Med.* **2015**, *48*, 573−580.

(16) Tyndall, J. A.; Gerona, R.; De Portu, G.; Trecki, J.; Elie, M. C.; Lucas, J.; Slish, J.; Rand, K.; Bazydlo, L.; Holder, M.; Ryan, M. F.; Myers, P.; Iovine, N.; Plourde, M.; Weeks, E.; Hanley, J. R.; Endres, G.; St Germaine, D.; Dobrowolski, P. J.; Schwartz, M. An outbreak of acute delirium from exposure to the synthetic cannabinoid AB-CHMINACA. *Clin. Toxicol.* **2015**, *53*, 950−956.

(17) Angerer, V.; Jacobi, S.; Franz, F.; Auwarter, V.; Pietsch, J. Three fatalities associated with the synthetic cannabinoids 5F-ADB, 5F-PB-22, and AB-CHMINACA. *Forensic Sci. Int.* **2017**, *281*, e9−e15.

(18) Adams, A. J.; Banister, S. D.; Irizarry, L.; Trecki, J.; Schwartz, M.; Gerona, R. "Zombie" Outbreak Caused by the Synthetic Cannabinoid AMB-FUBINACA in New York. *N. Engl. J. Med.* **2017**, *376*, 235−242.

(19) Kasper, A. M.; Ridpath, A. D.; Gerona, R. R.; Cox, R.; Galli, R.; Kyle, P. B.; Parker, C.; Arnold, J. K.; Chatham-Stephens, K.; Morrison, M. A.; Olayinka, O.; Preacely, N.; Kieszak, S. M.; Martin, C.; Schier, J. G.; Wolkin, A.; Byers, P.; Dobbs, T. Severe illness associated with reported use of synthetic cannabinoids: a public health investigation (Mississippi, 2015). *Clin. Toxicol.* **2019**, *57*, 10−18.

(20) Hermanns-Clausen, M.; Muller, D.; Kithinji, J.; Angerer, V.; Franz, F.; Eyer, F.; Neurath, H.; Liebetrau, G.; Auwarter, V. Acute side effects after consumption of the new synthetic cannabinoids AB-CHMINACA and MDMB-CHMICA. *Clin. Toxicol.* **2018**, *56*, 404−411.

(21) Uchiyama, N.; Shimokawa, Y.; Matsuda, S.; Kawamura, M.; Kikura-Hanajiri, R.; Goda, Y. Two new synthetic cannabinoids, AM-

2201 benzimidazole analog (FUBIMINA) and (4-methylpiperazin-1-yl)(1-pentyl-1H-indol-3-yl)methanone (MEPIRAPIM), and three phenethylamine derivatives, 25H-NBOMe 3,4,5-trimethoxybenzyl analog, 25B-NBOMe, and 2C-N-NBOMe, identified in illegal products. *Forensic Toxicol.* **2014**, *32*, 105−115.

(22) Adam, J. M.; Cairns, J.; Caulfield, W.; Cowley, P.; Cumming, I.; Easson, M.; Edwards, D.; Ferguson, M.; Goodwin, R.; Jeremiah, F.; Kiyoi, T.; Mistry, A.; Moir, E.; Morphy, R.; Tierney, J.; York, M.; Baker, J.; Cottney, J. E.; Houghton, A. K.; Westwood, P. J.; Walker, G. Design, synthesis, and structure−activity relationships of indole-3-carboxamides as novel water soluble cannabinoid CB1 receptor agonists. *MedChemComm* **2010**, *1*, 54−60.

(23) Kiyoi, T.; York, M.; Francis, S.; Edwards, D.; Walker, G.; Houghton, A. K.; Cottney, J. E.; Baker, J.; Adam, J. M. Design, synthesis, and structure−activity relationship study of conformationally constrained analogs of indole-3-carboxamides as novel CB1 cannabinoid receptor agonists. *Bioorg. Med. Chem. Lett.* **2010**, *20*, 4918−4921.

(24) European Monitoring Centre for Drugs and Drug Addiction. In *EMCDDA−Europol 2014 Annual Report on the implementation of Council Decision 2005/387/JHA, Implementation reports*; Publications Office of the European Union: Luxembourg; 2015, DOI: DOI: 10.2810/112317.

(25) Qian, Z.; Jia, W.; Li, T.; Hua, Z.; Liu, C. Identification and analytical characterization of four synthetic cannabinoids ADB-BICA, NNL-1, NNL-2, and PPA(N)-2201. *Drug Test. Anal.* **2017**, *9*, 51−60.

(26) National Forensic Laboratory Slovenia. 2017, Analytical report 5F-BEPIRAPIM (C25H30FN3O) 3-(4-benzylpiperazine-1-carbonyl)-1-(5-fluoropentyl)-1H-indole, Ljubljana, Slovenia. Available at: https://www.policija.si/apps/nfl_response_web/0_Analytical_Reports_final/5F-Bepirapim-ID-1770-17_report.pdf (accessed 11 July, 2021).

(27) Mochizuki, A.; Nakazawa, H.; Adachi, N.; Takekawa, K.; Shojo, H. Identification and quantification of mepirapim and acetyl fentanyl in authentic human whole blood and urine samples by GC-MS/MS and LC-MS/MS. *Forensic Toxicol.* **2018**, *36*, 81−87.

(28) Mochizuki, A.; Nakazawa, H.; Adachi, N.; Takekawa, K.; Shojo, H. Postmortem distribution of mepirapim and acetyl fentanyl in biological fluid and solid tissue specimens measured by the standard addition method. *Forensic Toxicol.* **2019**, *37*, 27−33.

(29) Banister, S. D.; Kevin, R. C.; Martin, L.; Adams, A.; Macdonald, C.; Manning, J. J.; Boyd, R.; Cunningham, M.; Stevens, M. Y.; McGregor, I. S.; Glass, M.; Connor, M.; Gerona, R. R. The chemistry and pharmacology of putative synthetic cannabinoid receptor agonist (SCRA) new psychoactive substances (NPS) 5F-PY-PICA, 5F-PY-PINACA, and their analogs. *Drug Test. Anal.* **2019**, *11*, 976−989.

(30) Zuurman, L.; Passier, P.; de Kam, M. L.; Kleijn, H. J.; Cohen, A. F.; van Gerven, J. M. A. Pharmacodynamic and pharmacokinetic effects of the intravenously administered CB1 receptor agonist Org 28611 in healthy male volunteers. *J. Psychopharmacol.* **2009**, *23*, 633−644.

(31) You, H.; Gadotti, V. M.; Petrov, R. R.; Zamponi, G. W.; Diaz, P. Functional Characterization and Analgesic Effects of Mixed Cannabinoid Receptor/T-Type Channel Ligands. *Mol. Pain* **2011**, *7*, 1744−8069.

(32) Bladen, C.; McDaniel, S. W.; Gadotti, V. M.; Petrov, R. R.; Berger, N. D.; Diaz, P.; Zamponi, G. W. Characterization of novel cannabinoid based T-type calcium channel blockers with analgesic effects. *ACS Chem. Neurosci.* **2015**, *6*, 277−287.

(33) Bean, B. P. Classes of Calcium Channels in Vertebrate Cells. *Annu. Rev. Physiol.* **1989**, *51*, 367−384.

(34) Ertel, E. A.; Campbell, K. P.; Harpold, M. M.; Hofmann, F.; Mori, Y.; Perez-Reyes, E.; Schwartz, A.; Snutch, T. P.; Tanabe, T.; Birnbaumer, L.; Tsien, R. W.; Catterall, W. A. Nomenclature of Voltage-Gated Calcium Channels. *Neuron* **2000**, *25*, 533−535.

(35) Perez-Reyes, E. Molecular Physiology of Low-Voltage-Activated T-type Calcium Channels. *Physiol. Rev.* **2003**, *83*, 117−161.

(36) Catterall, W. A. Voltage-Gated Calcium Channels. *Cold Spring Harbor Perspect. Biol.* **2011**, *3*, a003947.

(37) Nowycky, M. C.; Fox, A. P.; Tsien, R. W. Three types of neuronal calcium channel with different calcium agonist sensitivity. *Nature* **1985**, *316*, 440−443.

(38) Iftinca, M. C.; Zamponi, G. W. Regulation of neuronal T-type calcium channels. *Trends Pharmacol. Sci.* **2009**, *30*, 32−40.

(39) Huguenard, J.; Prince, D. A novel T-type current underlies prolonged Ca(2+)-dependent burst firing in GABAergic neurons of rat thalamic reticular nucleus. *J. Neurosci.* **1992**, *12*, 3804−3817.

(40) Weiss, N.; Zamponi, G. W. Control of low-threshold exocytosis by T-type calcium channels. *Biochim. Biophys. Acta, Biomembr.* **2013**, *1828*, 1579−1586.

(41) Weiss, N.; Zamponi, G. W. Genetic T-type calcium channelopathies. *J. Med. Genet.* **2020**, *57*, 1−10.

(42) Weiss, N.; Zamponi, G. W. T-Type Channel Druggability at a Crossroads. *ACS Chem. Neurosci.* **2019**, *10*, 1124−1126.

(43) Zamponi, G. W. Targeting voltage-gated calcium channels in neurological and psychiatric diseases. *Nat. Rev. Drug Discovery* **2016**, *15*, 19−34.

(44) Nam, G. T-type calcium channel blockers: a patent review (2012−2018). *Expert Opin. Ther. Pat.* **2018**, *28*, 883−901.

(45) Snutch, T. P.; Zamponi, G. W. Recent advances in the development of T-type calcium channel blockers for pain intervention. *Br. J. Pharmacol.* **2018**, *175*, 2375−2383.

(46) Ziegler, D.; Duan, W. R.; An, G.; Thomas, J. W.; Nothaft, W. A randomized double-blind, placebo-, and active-controlled study of T-type calcium channel blocker ABT-639 in patients with diabetic peripheral neuropathic pain. *Pain* **2015**, *156*, 2013−2020.

(47) Gadotti, V. M.; Kreitinger, J. M.; Wageling, N. B.; Budke, D.; Diaz, P.; Zamponi, G. W. Cav3.2 T-type calcium channels control acute itch in mice. *Mol. Brain* **2020**, *13*, No. 119.

(48) Gadotti, V. M.; Zamponi, G. W. Ethosuximide inhibits acute histamine- and chloroquine-induced scratching behavior in mice. *Mol. Brain* **2021**, *14*, No. 46.

(49) Walker, J. M.; Hohmann, A. G. Cannabinoid Mechanisms of Pain Suppression. In *Cannabinoids*, Pertwee, R. G., Ed.; Springer Berlin Heidelberg: Berlin, Heidelberg, 2005*168*; pp 509−554.

(50) Trotter, B. W.; Nanda, K. K.; Burgey, C. S.; Potteiger, C. M.; Deng, J. Z.; Green, A. I.; Hartnett, J. C.; Kett, N. R.; Wu, Z.; Henze, D. A.; Della Penna, K.; Desai, R.; Leitl, M. D.; Lemaire, W.; White, R. B.; Yeh, S.; Urban, M. O.; Kane, S. A.; Hartman, G. D.; Bilodeau, M. T. Imidazopyridine CB2 agonists: optimization of CB2/CB1 selectivity and implications for in vivo analgesic efficacy. *Bioorg. Med. Chem. Lett.* **2011**, *21*, 2354−2358.

(51) Gifford, A. N.; Bruneus, M.; Gatley, S. J.; Lan, R.; Makriyannis, A.; Volkow, N. D. Large receptor reserve for cannabinoid actions in the central nervous system. *J. Pharmacol. Exp. Ther.* **1999**, *288*, 478−483.

(52) Cannaert, A.; Sparkes, E.; Pike, E.; Luo, J. L.; Fang, A.; Kevin, R. C.; Ellison, R.; Gerona, R.; Banister, S. D.; Stove, C. P. Synthesis and in Vitro Cannabinoid Receptor 1 Activity of Recently Detected Synthetic Cannabinoids 4F-MDMB-BICA, 5F-MPP-PICA, MMB-4en-PICA, CUMYL-CBMICA, ADB-BINACA, APP-BINACA, 4F-MDMB-BINACA, MDMB-4en-PINACA, A-CHMINACA, 5F-AB-P7AICA, 5F-MDMB-P7AICA, and 5F-AP7AICA. *ACS Chem. Neurosci.* **2020**, *11*, 4434−4446.

(53) Bladen, C.; Mirlohi, S.; Santiago, M.; Longworth, M.; Kassiou, M.; Banister, S.; Connor, M. Modulation of human T-type calcium channels by synthetic cannabinoid receptor agonists in vitro. *Neuropharmacology* **2021**, *187*, No. 108478.

(54) Kevin, R. C.; Anderson, L.; McGregor, I. S.; Boyd, R.; Manning, J. J.; Glass, M.; Connor, M.; Banister, S. D. CUMYL-4CN-BINACA Is an Efficacious and Potent Pro-Convulsant Synthetic Cannabinoid Receptor Agonist. *Front. Pharmacol.* **2019**, *10*, 595.

(55) Gatch, M. B.; Forster, M. J. Cannabinoid-like effects of five novel carboxamide synthetic cannabinoids. *Neurotoxicology* **2019**, *70*, 72−79.

(56) Wilson, C. D.; Tai, S.; Ewing, L.; Crane, J.; Lockhart, T.; Fujiwara, R.; Radominska-Pandya, A.; Fantegrossi, W. E. Convulsant Effects of Abused Synthetic Cannabinoids JWH-018 and 5F-AB-PINACA Are Mediated by Agonist Actions at CB1 Receptors in Mice. *J. Pharmacol. Exp. Ther.* **2019**, *368*, 146−156.

(57) Gatch, M. B.; Tourigny, A.; Shetty, R. A.; Forster, M. J. Behavioral pharmacology of five novel synthetic cannabinoids. *Behav. Pharmacol.* **2022**, *33*, 175−183.
(58) Banister, S. D.; Wilkinson, S. M.; Longworth, M.; Stuart, J.; Apetz, N.; English, K.; Brooker, L.; Goebel, C.; Hibbs, D. E.; Glass, M.; Connor, M.; McGregor, I. S.; Kassiou, M. The synthesis and pharmacological evaluation of adamantane-derived indoles: cannabimimetic drugs of abuse. *ACS Chem. Neurosci.* **2013**, *4*, 1081−1092.
(59) Hua, T.; Li, X.; Wu, L.; Iliopoulos-Tsoutsouvas, C.; Wang, Y.; Wu, M.; Shen, L.; Brust, C. A.; Nikas, S. P.; Song, F.; Song, X.; Yuan, S.; Sun, Q.; Wu, Y.; Jiang, S.; Grim, T. W.; Benchama, O.; Stahl, E. L.; Zvonok, N.; Zhao, S.; Bohn, L. M.; Makriyannis, A.; Liu, Z.-J. Activation and Signaling Mechanism Revealed by Cannabinoid Receptor-Gi Complex Structures. *Cell* **2020**, *180*, 655−665.e18.
(60) Halgren, T. A. Identifying and characterizing binding sites and assessing druggability. *J. Chem. Inf. Model.* **2009**, *49*, 377−389.
(61) Halgren, T. New method for fast and accurate binding-site identification and analysis. *Chem. Biol. Drug Des.* **2007**, *69*, 146−148.
(62) Adam, J. M.; Cairns, J.; Caulfield, W.; Cowley, P.; Cumming, I.; Easson, M.; Edwards, D.; Ferguson, M.; Goodwin, R.; Jeremiah, F.; et al.*et al.* Design, synthesis, and structure−activity relationships of indole-3-carboxamides as novel water soluble cannabinoid CB1 receptor agonists. *MedChemComm* **2010**, *1*, 54−60.
(63) Ametovski, A.; Cairns, E. A.; Grafinger, K. E.; Cannaert, A.; Deventer, M. H.; Chen, S.; Wu, X.; Shepperson, C. E.; Lai, F.; Ellison, R.; Gerona, R.; Blakey, K.; Kevin, R.; McGregor, I. S.; Hibbs, D. E.; Glass, M.; Stove, C.; Auwärter, V.; Banister, S. D. NNL-3: A Synthetic Intermediate or a New Class of Hydroxybenzotriazole Esters with Cannabinoid Receptor Activity? *ACS Chem. Neurosci.* **2021**, *12*, 4020−4036.
(64) Abdel-Magid, A. F.; Carson, K. G.; Harris, B. D.; Maryanoff, C. A.; Shah, R. D. Reductive Amination of Aldehydes and Ketones with Sodium Triacetoxyborohydride. Studies on Direct and Indirect Reductive Amination Procedures. *J. Org. Chem.* **1996**, *61*, 3849−3862.
(65) Finlay, D. B.; Cawston, E. E.; Grimsey, N. L.; Hunter, M. R.; Korde, A.; Vemuri, V. K.; Makriyannis, A.; Glass, M. Galphas signalling of the CB1 receptor and the influence of receptor number. *Br. J. Pharmacol.* **2017**, *174*, 2545−2562.
(66) Grimsey, N. L.; Goodfellow, C. E.; Dragunow, M.; Glass, M. Cannabinoid receptor 2 undergoes Rab5-mediated internalization and recycles via a Rab11-dependent pathway. *BBA, Biochim. Biophys. Acta, Mol. Cell Res.* **2011**, *1813*, 1554−1560.
(67) Knapman, A.; Santiago, M.; Du, Y. P.; Bennallack, P. R.; Christie, M. J.; Connor, M. A continuous, fluorescence-based assay of mu-opioid receptor activation in AtT-20 cells. *J. Biomol. Screening* **2013**, *18*, 269−276.
(68) Feng, Z.-P.; Doering, C. J.; Winkfein, R. J.; Beedle, A. M.; Spafford, J. D.; Zamponi, G. W. Determinants of inhibition of transiently expressed voltage-gated calcium channels by omega-conotoxins GVIA and MVIIA. *J. Biol. Chem.* **2003**, *278*, 20171−20178.
(69) Banister, S. D.; Olson, A.; Winchester, M.; Stuart, J.; Edington, A. R.; Kevin, R. C.; Longworth, M.; Herrera, M.; Connor, M.; McGregor, I. S.; Gerona, R. R.; Kassiou, M. The chemistry and pharmacology of synthetic cannabinoid SDB-006 and its regioisomeric fluorinated and methoxylated analogs. *Drug Test. Anal.* **2018**, *10*, 1099−1109.
(70) Krishna Kumar, K.; Shalev-Benami, M.; Robertson, M. J.; Hu, H.; Banister, S. D.; Hollingsworth, S. A.; Latorraca, N. R.; Kato, H. E.; Hilger, D.; Maeda, S.; et al.*et al.* Structure of a signaling cannabinoid receptor 1-G protein complex. *Cell* **2019**, *176*, 448−458.e12.
(71) Xing, C.; Zhuang, Y.; Xu, T.-H.; Feng, Z.; Zhou, X. E.; Chen, M.; Wang, L.; Meng, X.; Xue, Y.; Wang, J.; Liu, H.; McGuire, T. F.; Zhao, G.; Melcher, K.; Zhang, C.; Xu, H. E.; Xie, X.-Q. Cryo-EM Structure of the Human Cannabinoid Receptor CB2-Gi Signaling Complex. *Cell* **2020**, *180*, 645−654.e13.
(72) Madhavi Sastry, G.; Adzhigirey, M.; Day, T.; Annabhimoju, R.; Sherman, W. Protein and ligand preparation: parameters, protocols, and influence on virtual screening enrichments. *J. Comput.-Aided Mol. Des.* **2013**, *27*, 221−234.
(73) Shelley, J. C.; Cholleti, A.; Frye, L. L.; Greenwood, J. R.; Timlin, M. R.; Uchimaya, M. Epik: a software program for pK a prediction and protonation state generation for drug-like molecules. *J. Comput.-Aided Mol. Des.* **2007**, *21*, 681−691.
(74) Olsson, M. H. M.; Søndergaard, C. R.; Rostkowski, M.; Jensen, J. H. PROPKA3: consistent treatment of internal and surface residues in empirical p K a predictions. *J. Chem. Theory Comput.* **2011**, *7*, 525−537.
(75) Jorgensen, W. L.; Maxwell, D. S.; Tirado-Rives, J. Development and testing of the OPLS all-atom force field on conformational energetics and properties of organic liquids. *J. Am. Chem. Soc.* **1996**, *118*, 11225−11236.
(76) *LigPrep*; Schrödinger, LLC: New York, NY, 2021.
(77) Sherman, W.; Day, T.; Jacobson, M. P.; Friesner, R. A.; Farid, R. Novel procedure for modeling ligand/receptor induced fit effects. *J. Med. Chem.* **2006**, *49*, 534−553.

https://doi.org/10.1021/acschemneuro.1c00822
ACS Chem. Neurosci. 2022, 13, 1395−1409